Review Article

ADVANCED PHOTONICS

Multifunctional integration on optical fiber tips: challenges and opportunities

Yifeng Xiong and Fei Xu*
Nanjing University, College of Engineering and Applied Sciences, Nanjing, China

Abstract. The flat endface of an optical fiber tip is an emerging light-coupled microscopic platform that combines fiber optics with planar micro- and nanotechnologies. Since different materials and structures are integrated onto the endfaces, optical fiber tip devices have miniature sizes, diverse integrated functions, and low insertion losses, making them suitable for all-optical networks. In recent decades, the increasing demand for multifunctional optical fibers has created opportunities to develop various structures on fiber tips. Meanwhile, the unconventional shape of optical fibers presents challenges involving the adaptation of standard planar micro- and nanostructure preparation strategies for fiber tips. In this context, researchers are committed to exploring and optimizing fiber tip manufacturing techniques, thereby paving the way for future integrated all-fiber devices with multifunctional applications. First, we present a broad overview of current fabrication technologies, classified as "top-down," "bottom-up," and "material transfer" methods, for patterning optical fiber tips. Next, we review typical structures integrated on fiber tips and their known and potential applications, categorized with respect to functional structure configurations, including "optical functionalization" and "electrical integration." Finally, we discuss the prospects for future opportunities involving multifunctional integrated fiber tips.

Keywords: optical fibers; fiber tips; optical devices; nanotechnology; micro-optics; nano-optics.

Received Aug. 6, 2020; revised manuscript received Sep. 20, 2020; accepted for publication Sep. 25, 2020; published online Nov. 4, 2020.

[DOI: 10.1117/1.AP.2.6.064001]

1 Introduction

Since 1966, when K. C. Kao and G. A. Hockham proposed the idea of low-optical-loss glass fibers, the invention of ultralow-loss silica optical fibers has contributed to the rapid development of numerous fields, including communications, sensing, lasing, and imaging. The unique properties of optical fibers, including their small size, ultrahigh aspect ratio, high mechanical robustness, immunity to electromagnetic interference, and high biocompatibility, facilitate their application in various environments such as remote distances, confined spaces, and even harsh environments with extremes of temperature, pressure, corrosion, and electromagnetic field.

However, the limitations of the material characteristics (most often SiO_2) and geometry structures of optical fibers hinder further applications. To solve this problem, researchers have attempted to integrate different materials and structures into optical fiber configurations in the fiber-drawing, with the aim of producing fibers that can see, hear, sense, and communicate.[1–12] The field of "multimaterial fibers" arouses great industrial interest, while it also faces some technological challenges. Alternatively, there is thriving research momentum in innovating commercially available optical fibers and developing lab-on-fiber (LOF) technology.

In recent decades, numerous designs for LOF devices have been reported; these can be classified with respect to their approach to light–matter interactions and divided into two types: waveguide integration and fiber tip integration. Waveguide integration includes the integration of functional materials on the outer cylindrical surface of optical fibers (such as microfibers,[13,14] unclad fibers,[15,16] and D-shaped fibers[15,17,18]), and the function performed within the fiber [e.g., fiber Bragg gratings[19] and holey structures characteristic of photonic crystal (PC) fibers[20]]. Although these devices achieve light–matter interactions over long distances and large areas, they often suffer from certain drawbacks such as large device size, high insertion

*Address all correspondence to Fei Xu, feixu@nju.edu.cn

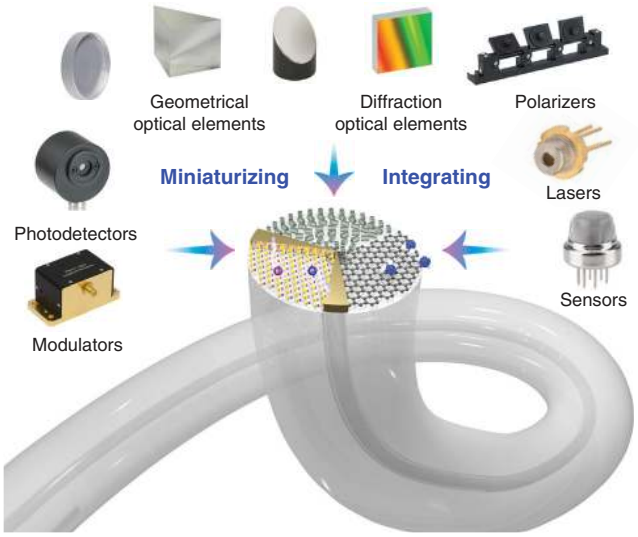

Fig. 1 Multifunctional integration on optical fiber tips. Traditional optical, electrical, acoustic, thermal, biological, and chemical structures have been miniaturized and integrated onto optical fiber tips.

loss, and incompatibility with traditional planar micro- and nanofabrication technologies. Fiber tip integration refers to the integration of functional materials and structures on the microscale plane of the fiber endface, which provides an inherently light-coupled platform for micro- and nanotechnologies. Fiber tip devices have been emerging as new integrated plug and play components for optical networks (Fig. 1); they have small device volumes and low insertion losses but suffer limitations of short light–matter interaction distance and small sensing area as a trade-off. Moreover, the unconventional shape of optical fibers, which have a small diameter and a large aspect ratio, presents challenges when adapting standard planar nanostructure fabrication strategies for fiber tips.

In response to these challenges, researchers used two principal approaches. In the first approach, the nanomaterials or nanostructures are fabricated on a planar substrate using standard materials synthesis processes and planar nanotechnologies. The main challenge facing this approach is the subsequent transfer of the prepared structure onto the fiber tip and ensuring that the completed structure is bonded firmly to the fiber tip and aligned precisely to the fiber core. This approach is elaborated on later as part of the discussion on material transfer methodologies. The second approach focuses on fabricating the nanomaterials or nanostructure on the fiber tips directly via optimized fabrication strategies, which can be categorized as either "top down" or "bottom up" methodologies.

So far, there have been several review papers on LOF technology, which have provided a timely overview on many aspects ranging from materials and mechanisms to fabrication techniques as well as device configuration designs, with the aim of realizing integrated and miniaturized all-fiber systems.[21–26] As the research continues, the multifunctional fiber tips have broader application prospects and get closer to practical applications. It is nontrivial to give a systematic overview of their pros and cons for fabrication techniques and a detailed classification on the related fiber tip applications, considering the optical and optoelectrical functional integration. In addition to the micro/nanostructure integration, nanomaterials for building functionalized optical fiber tips are introduced, which has rarely been summarized systematically in previous reviews.

In this paper, we first review the main fabrication technologies reported thus far for multifunctional fiber tip devices, including mechanical processing, chemical etching, focused ion beam (FIB) etching, laser processing, lithography methods, self-assembly (SA), and chemical vapor deposition (CVD)/physical vapor deposition (PVD) processing, as well as material transfer methods. Subsequently, we overview some of the most typical and interesting structures applied to fiber tips and present a detailed overview of the related devices and their general field of applications. Finally, we review the ongoing development of strategies aiming at building multifunctional fiber tip devices with improved integration and increased application diversity.

2 Fabrication Technologies

2.1 Top-Down Methodologies

Top-down fabrication is a subtractive process in which material is removed gradually from the bulk to form micro/nanometer-size structures with a controlled shape and size. As shown in Fig. 2, typical examples of top-down approaches are discussed in this section, including FIB etching, plasma etching (PE), photolithography, and electron-beam lithography (EBL). In general, most top-down fabrication methods are not suitable for production on a very large scale, owing to the long duration and high costs associated with these methods. Nevertheless, they represent some of the most common approaches used to produce controlled two-dimensional (2D) and three-dimensional (3D) periodic features on substrates.

On the platform of the fiber tip, conventional fabrication technologies typically require optimization. For example, the optical fiber has a small diameter and a large aspect ratio, which

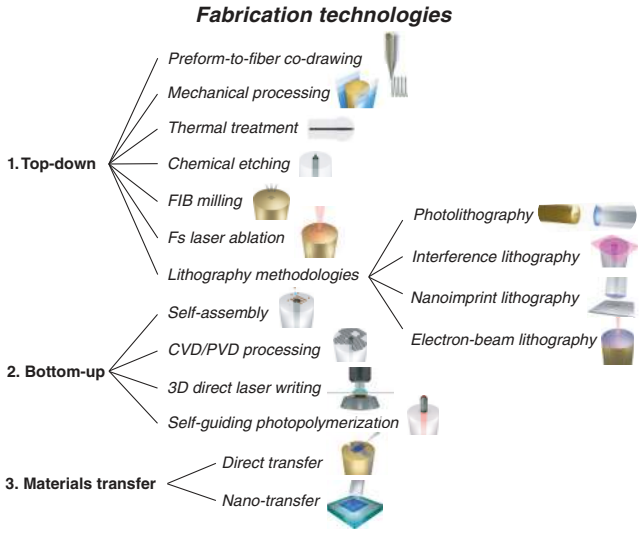

Fig. 2 Tree diagram of the fabrication technologies for LOF-tip. The "top down" and "bottom up" methodologies involve fabricating the nanomaterials or nanostructure on the fiber tips directly, while the material transfer methodologies involve fabricating the nanomaterials or nanostructure separately on a planar substrate before transferring the prepared structure onto the fiber tips.

poses challenges for traditional spin-coating of the photoresist for lithography fabrication. Silica optical fibers without a protection polymer cladding are usually fragile, making controlling the fiber and handling it using the fabrication equipment incredibly difficult. In recent decades, many fabrication technologies have been transferred successfully from planar systems onto optical fibers. A selection of these methods is discussed hereafter.

2.1.1 Preform-to-fiber co-drawing method

The direct homothetic preform-to-fiber co-drawing method can produce microstructured "multimaterial fibers" combined with a variety of materials with disparate electrical, optical, and mechanical properties by thermal drawing. This method could be applied to a wide range of polymers, glasses, polymer composites, metals, semiconductors, and dielectrics, which greatly improves the scope of applications for optical fibers.[1–12,27–30]

This multimaterial thermal drawing method takes advantage of the scalability of fiber processing that enables complex and multiple functionalities within optical fibers. Nevertheless, manufacturing the internal architecture of optical fibers is a relatively complex and expensive process that is limited by the compatible materials and special geometries available.

2.1.2 Mechanical processing

Mechanical processing is a simple method for optical fiber tip fabrication, which includes some basic optical fiber machining such as polishing. It can quickly and easily process the fiber tips on a large scale, but obtaining fine structures is difficult. In the 1990s, fiber tips were roughened using a piece of polish paper to obtain rough fiber endfaces, and then a metallic film was coated on this rough surface to support plasmonic resonances to produce fibers suitable for surface-enhanced Raman scattering (SERS) sensors.[31–33] Thereafter, fiber tips were polished into different shapes, such as fiber microaxicons, using polishing techniques.[34] Moreover, polishing techniques were also used to process metal structures on optical fibers.[35–37] As shown in Fig. 3, Chen et al.[38] fabricated electrodes on optical fibers using lapping films and tapered tungsten needles to remove a portion of the precoated gold film on the fiber sidewall and facet.

Mechanical assembly is an approach widely used to fabricate optomechanical devices, where microoptomechanical cavities were assembled on the optical fiber tips. Typical optomechanical cavities include simple cantilevers or membranes sustained by cantilevers, placed suspended on the optical fiber endfaces, demonstrating the application of accelerometers,[39] optical force transducers for mapping tissue mechanics,[40] local dynamic mechanical measurement,[41] as well as seismic sensors.[42]

In addition, the introduction of microrobot arms inside the scanning electron microscope (SEM) vacuum chamber provides possibilities for cutting, etching, folding, assembling, and then welding thin membranes on top of optical fiber tips. Under this approach, Rauch et al.[43] fabricated a small microhouse on an optical fiber endface, which was carved by FIB, assembled by origami, and welded by microrobot nanofactory. Although the shortcomings of fabricating them reliably, reproducibly, and stably remain, it is a potential way to realize several 3D micro- and nanostructures on fiber tips.

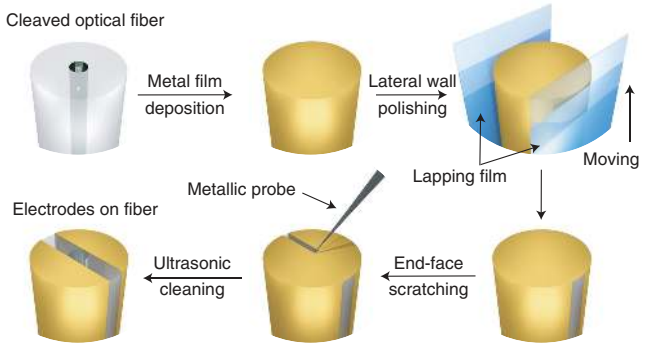

Fig. 3 Schematic of the mechanical fabrication processes for electrodes on an optical fiber tip.[38] First, lapping films are used to remove a portion of the precoated gold from the fiber sidewall. Then, an electrode on a fiber facet is fabricated by scratching the gold layer using a tapered tungsten needle.

2.1.3 Thermal treatment

Thermal treatment includes some basic optical fiber operations such as splicing and melting. Splicing is an efficient way to fabricate functional fiber tips quickly. For example, optical fiber Fabry–Perot (FP) cavities can be fabricated easily by splicing a cleaved optical fiber and a short capillary and subsequently laminating a thin film on the surface to form an optical microcavity that can sense sound, vibration, and pressure.[44–49] In addition, both coreless and hollow fibers as well as certain fiber fusion structures (such as bubbles) have also been used to form resonant cavities.[50]

Owing to the surface tension of silica, microspheres can be easily created at the fiber tip by melting it. The high temperatures required here can be provided by a CO_2 laser, high temperature flame, or the arc discharge of a fusion splicer machine.[51] In recent decades, microspheres on fiber tips have been deployed as microlenses, resonators in a range of sensing applications.[52–55]

2.1.4 Chemical etching

Silica and glass optical fibers can be chemically etched via a buffered hydrogen fluoride solution containing a certain percentage of hydrofluoric acid (HF) and an aqueous solution of ammonium fluoride (NH_4F). The etching speeds relating to fiber cores and claddings depend on the doping materials and the volume ratio of the etching solution; they can also be controlled via the etching time, HF concentration, and the temperature of the solution.

Over recent decades, chemical etching methods have been used frequently to process functional structures on optical fibers.[56–58] When the etching speed for fiber cladding is faster than that for the fiber core, a cone-shaped structure is formed on the top of the fiber. Thus, Eisenstein and Vitello[59] proposed a conical microlens on a fiber tip to reduce coupling loss between a laser diode and a single-mode fiber. Optical near-field microscopic probes with high transmission efficiency were demonstrated using a double taper-etched fiber tip structure coated with a layer of metal.[60–63] Adopting a similar approach, Maruyama et al.[64] reported a pencil-shaped nanometer-sized optical fiber electrode for scanning optical and electrochemical microscopy. Recently, Wang et al.[65] fabricated 2D light-guiding arrays formed from mechanically compliant glass nanospikes, measuring 100 μm in length, by dipping a multicore fiber into dilute nitric acid.

Moreover, chemical etching has also been used to fabricate holes in the fiber core using a faster etch speed for the fiber core than for the fiber cladding.[66] For example, Zheng et al.[67] produced an optical fiber current sensor based on a graphene nanoelectromechanical system (NEMS), in which a graphene film covered the hole on a chemically etched fiber tip and two gold electrodes were placed on opposite sides of the tip.

In general, chemical etching methods can quickly and effectively corrode optical fiber materials, which facilitate large-scale production. Different fiber tip structures can be obtained depending on the selection of the optical fiber doping materials and the etching conditions. However, chemical etching struggles to process highly complex structures accurately.

2.1.5 Focused ion beam milling

FIB milling is a typical top-down approach that uses a high-energy FIB to remove atoms from the sample surface, thereby allowing the direct patterning of materials ranging from fiber glass to metals to create a desired micro/nanoscale surface topography.

Thus far, many studies have proposed FIB milling patterns on fiber tips. In the mid-2000s, FIB milling was used predominantly to etch fiber glass on the fiber tip, aiming at carving the optical fiber tip to miniaturize optical and mechanical devices.[68] For example, Schiappelli et al.[69] demonstrated an FIB fabricated microlens on the fiber tip to realize efficient optical coupling between a single-mode fiber and a waveguide. Iannuzzi et al.[70,71] used FIB to achieve an atomic force microscope (AFM) based on a microcantilever on a fiber tip. By properly shaping the fiber tip of an annular-core fiber, Liberale et al.[72] demonstrated miniaturized all-fiber optical tweezers, which is promising for optical 3D trapping and manipulation.

In addition to the direct etching of fiber glass on fiber tips, fiber devices based on FIB-fabricated metallic nanostructures have been proposed to support surface plasmons.[73–75] For instance, Dhawan et al.[76,77] used FIB milling to fabricate ordered arrays of nanoholes on gold-coated cleaved or tapered optical fibers, and they demonstrated the sensing of the refractive index (RI). Recently, Principe et al.[78] reported an optical fiber "metatip" (MT) by integrating a phase-gradient plasmonic metasurface on the fiber tip.

Moreover, FIB processing has been employed to template optical fiber tips. After patterning the fiber glass, different materials can be deposited to form hybrid nanostructures that serve multiple applications.[79] For example, Micco et al.[80] milled the fiber glass directly and subsequently deposited a high RI material overlay, thus forming a "double-layer" PC slab and supporting the guided resonance.

In general, FIB milling exploits the advantages of maskless patterning; however, it also suffers from some intrinsic drawbacks. First, it is hard to avoid creating patterned structures with angled sidewalls, especially when the size of the etched structure is large. Second, although a thin metal film is predeposited on optical fibers, ion doping of the substrate is unavoidable because of the poor conductivity of optical fibers. Furthermore, FIB milling is time-consuming, and the processing area is limited for each fabrication step.[23]

2.1.6 Femtosecond laser ablation

Femtosecond (fs) laser ablation utilizes a similar processing principle as FIB milling. The focused fs laser has a very high instantaneous power, which can quickly and effectively pattern nanostructures with minimal impact on the surrounding materials. While the fs laser etching process is generally faster and cheaper than those based on FIB milling, the processing accuracy is challenging for further applications. Faced with this challenge, fs laser two-/multiphoton polymerization methods have been developed, which are discussed in the section on bottom-up methodologies.

In recent decades, several fs laser machining methods have been proposed. For example, fs lasers have been utilized to ablate fiber glass to create grating structures, Fresnel zone plate lenses, and rough surfaces on fiber endfaces to facilitate sensing, imaging, SERS, and many other applications.[81–84]

2.1.7 Lithography methodology

Lithography methods are powerful and precise approaches for micro- and nanofabrication, which are utilized widely in the fields of nanoelectronics and photonics. With the development of nanotechnology, lithography methods have progressed from conventional optical-based photolithography to newer technologies that use electron beams, x-rays, micro-ion beams, and focused lasers as radiation sources, which increase the precision of the transferred patterns significantly. A fiber endface can be regarded as a relatively large planar surface on which to embrace the lithography technologies, which were originally applied to planar substrates. However, owing to the shape of the optical fiber, applying the lithography process to the fiber endface also faces several challenges.

In general, obtaining a uniform resist layer on an optical fiber facet with a controllable thickness is one of the most important yet challenging procedures that form the lithography process. Lin and coworkers proposed the "dip and vibration" coating technique [Fig. 4(a)], in which the optical fiber was dipped into the resist solution and taken out to execute the mechanical vibration process. In the vibration procedure, the optical fiber was held by a fiber clamp and oriented to face directly upward. The resist layer thickness was controlled by adjusting the length of the fiber tip outside of the fiber clamp and the initial displacement of the fiber tip.[85–87]

Moreover, spin-coating is a traditional method for resist coating on planar substrates, which can control the thickness of coating layers precisely via the spinning time and rotation rate. However, the small diameter and large aspect ratio of the optical fiber make it difficult to adapt the traditional spin-coating method for application to optical fiber tips. One reason for this is that there is no commercial rotating chuck in which to hold fibers in a vertical direction. In addition, the spin-coating process typically produces edge beads around the perimeter of the substrates, which is especially obvious for small-sized substrates such as optical fiber endfaces. To overcome these

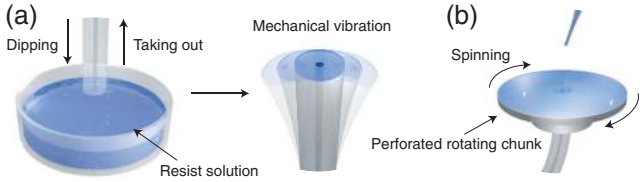

Fig. 4 Methods to obtain a thin photoresist film on optical fiber endfaces. (a) Schematic illustration of the "dip and vibration" method.[85–87] (b) Schematic illustration of the spin-coating method. The optical fiber is fixed to a perforated rotating chunk.[88]

difficulties, Consales et al.[88] adopted a customized rotating chuck to hold the optical fibers [Fig. 4(b)] and confirmed the uniform thickness of the spin-coated layer over an area with a diameter of ~50 to 60 μm over the fiber core. Furthermore, Feng et al.[89] proposed a fiber holder consisting of two brass half-cylinders with triangular grooves, in which the fibers were fixed by conductive carbon glue. The holder was then clamped by screws and polished to obtain a large smooth surface that included the optical fiber endfaces. For the most part, the large surface of the holder reduces the influence of edge beads forming during the spin-coating procedure, which benefits mass production.

After solving the resist coating problem, multiple lithography methods including photolithography, EBL, nanoimprint lithography (NIL), and interference lithography (IL) have been proposed for application to optical fiber endfaces; they are reviewed below.

Photolithography. Conventional photolithography involves the transfer of patterns from masks to planar substrates, which is comprised of the optical–chemical reaction of the photoresist and, subsequently, either chemical/physical etching or the metal coating method. The precise alignment of the mask and the optical fiber during the photolithography process is crucial. Most photolithography equipment is designed for planar substrates, which leads to compatibility issues with the vertically oriented optical fibers. Therefore, special processing is required to realize the conventional photolithography process for optical fiber endfaces.[90]

A number of studies describe attempts to pattern optical fiber facets using the photolithography method. For example, Johnson et al.[91] prepared a wafer consisting of tightly packed coreless fiber bundles and fabricated diffractive optical elements using photolithography. Conversely, Petrušis et al.[92] proposed an all-in-fiber photolithography technique, where the lithography mask was fabricated on an ultraviolet multimode fiber endface, which was aligned and brought into contact of another photoresist-coated fiber via a commercially available optical fiber splicing machine. Consequently, ultraviolet light was coupled from the opposite end of the mask fiber, and the pattern was transferred to the target fiber.

In addition to photolithography with a physical photomask, a maskless fabrication system for integrating microscale optical structures with fiber endfaces was proposed recently by Kim and Jeong.[93] This maskless UV exposure system used a digital micromirror device (DMD) as a variable photomask, which provided a spatial resolution of 2.2 μm for an exposed area of 245 μm × 185 μm.

Interference lithography. The IL technique allows a photoresist to record precise periodic interference patterns comprising two or more coherent light beams. In general, different array structures in one-, two-, or three-dimensions can be fabricated using different light beam combinations. For instance, Choi et al.[94] used the IL method to inscribe one- and two-dimensional surface relief gratings on an optical fiber endface covered with an azo polymer thin film layer. Following a similar approach, Feng et al.[95] fabricated optical fiber-based devices consisting of a ZnO waveguide and photoresist grating-structures. Alternatively, Yang et al.[96] used the IL method to pattern photoresist nanopillars on fiber endfaces and subsequently proposed an optical fiber SERS probe by etching the fiber and applying a coating of silver. The minimum processing resolution of IL is half of the light wavelength, and this represents the main drawback of the technique. In addition, the IL technique is only suitable for processing array structures.

Nanoimprint lithography. Nanoimprinting (NI) is a simple patterning technique that enables the user to produce large-area, high-resolution nanometer-scale patterns via the mechanical modification of materials, with low cost and high-throughput. Despite these advantages, when the predesigned pattern on the template has small dimensions, it is challenging to align the optical fibers precisely with the patterns during NI.

NI onto optical fiber endfaces can be categorized into two main approaches. Following one approach, the nanoimprint can be implemented directly on the thermally softened fiber tips of polymer fibers, polycrystalline silver-halide, chalcogenide optical fibers, and polymer layers on fibers.[97–102] Compared to common silica optical fibers, all of the optical fibers mentioned above are made of low transition temperature materials.

As shown in Fig. 5(a), optical fibers with low transition temperatures are aligned and placed in contact with the heated mold bearing the patterns. Then, the optical fiber is thermally softened, and the mechanical contact of the optical fiber and mold imposes both surface planarity and texture details onto the fiber endfaces. In this way, Sakata and Imada used a plastic optical fiber to imprint the patterns of concave lens cavities for efficient optical coupling directly. The temperature of the imprint mold was set to be 150°C to 155°C, and the lens cavities were filled with a high RI liquid resin after the imprinting process.[101] Sanghera et al.[99] adopted a similar approach to demonstrate a microstructured chalcogenide fiber tip with antireflective properties by NI at a temperature of 200°C to 240°C. The drawbacks of NI directly on fiber endfaces are the inherent limitations of the optical fiber materials and the distortion incurred during the thermal molding of the optical fibers.

Therefore, the NIL method has been proposed and applied to polymer precoated optical fiber endfaces. In contrast to lithography methods using focused light, electron beams, and many other radiation sources, the resolution of NIL depends

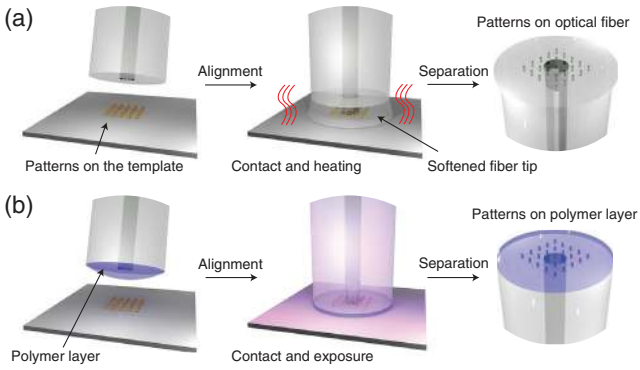

Fig. 5 Schematic illustration of the NI process of optical fibers. (a) NI process based on thermal softening. The optical fiber is aligned and placed in contact with the heated mold to transfer patterns onto the fiber tip. (b) NI process based on lithography. The optical fiber is precoated with polymer, then aligned, and placed in contact with the mold, with patterns transferred to the polymer layer via the exposure procedure.

predominantly on the accuracy of the template and thus is free from light diffraction or electron scattering. Moreover, the direct assembly of polymer layers onto fiber endfaces eliminates the need for further material transfer steps. As shown in Fig. 5(b), the optical fiber is coated with a layer of a light curable polymer, typically via the dip-coating method. Then, the optical fiber is aligned and placed into contact with the mold bearing the patterns, followed by the exposure procedure. The mechanical contact between the optical fiber and the mold imposes both surface planarity and texture structures onto the polymer layer.

In this context, periodic patterns with subwavelength dimensions have been fabricated successfully using NIL.[103–107] Micro-optical devices such as near-field probes have also been reported; such devices use NIL to fabricate functional optical transformers onto optical fiber endfaces.[108] These approaches necessitate a high precision multi-axis translation stage to align the small-sized optical fibers and the proportionally small-sized molds precisely. To surmount this problem, Kostovski et al.[109] utilized a technique using a single-axis linear stage for parallel, self-aligned, and portable optical fiber NIL. They employed a row of U-shaped grooves on the stage to confine the optical fibers, allowing them to self-align against the large-area curved mold, thus reducing the operation difficulty and increasing the throughput.

Electron-beam lithography. EBL is a powerful serial method for nanofabrication, whereby a beam of electrons is focused at the nanometer scale and scanned in arbitrary 2D geometries with an ultimate resolution of sub-10 nm. As with photolithography, electron irradiation modifies the electron beam resist chemically, finally forming the predesigned pattern after the development process. EBL procedures are afflicted by electrostatic charging issues caused by the electrically insulating nature of optical fiber materials; one solution to this is to deposit conductive layers on the fiber surface.[85,88,110] As shown in Fig. 6, there are two main fabrication approaches for patterning optical fiber endfaces using EBL. One approach first coats a layer of resist on a cleaved optical fiber and then deposits a thin metal layer to improve the conductivity of the optical fiber. After electron beam exposure, the precoated thin metal layer can be removed by etching methods such as reactive-ion etching. Then, the patterned electron beam resist layer is developed, which can be used directly as optical components,[88,111,112] or they can serve as masks for subsequent etching or lift-off procedures.[86,87,89,113] By contrast, the other approach first deposits a metal layer on a fiber and coats a layer of electron beam resist. After the EBL process, the pattern on the electron beam resist layer is transferred to the metal layer below using etching methods.

The EBL process provides a precise and versatile approach for integrating nanostructures such as photonic and plasmonic crystals onto optical fiber tips. The typical area that can be patterned with EBL is of the order of 100 μm × 100 μm, which corresponds to the dimensions of optical fibers. Nevertheless, EBL also suffers from some intrinsic drawbacks, such as the angled sidewalls of patterned structures and the time-consuming nature of the patterning process, which excludes it as a vehicle for mass production. EBL is also used to fabricate nanostructures on planar substrates that are then transferred to optical fiber endfaces; this is discussed later and referred to as the "nanotransfer method."

2.2 Bottom-Up Methodologies

Bottom-up fabrication is an additive process in which single atomic or molecular species are used to create self-assembled clusters with desired conformations. Bottom-up methodologies usually have low device production costs, which are an advantage for mass production; however, this is balanced against the sacrifice of precise control of the geometrical and physical parameters of the structures. There are numerous bottom-up methods for producing nanostructures, including sol–gel processing, SA, CVD, PVD, atomic layer deposition, 3D printing, and laser-induced photopolymerization.

For some of the bottom-up methods, such as SA and CVD, the optical fiber is regarded as a kind of silica substrate, which is compatible with the fabrication process. As for bottom-up methods such as conventional 3D printing, the fabrication technology is typically optimized for application on optical fibers, which is quite different than for the planar substrates. Moreover, the light waveguiding properties of the optical fiber are convenient for methods such as photopolymerization. In recent decades, many fabrication technologies have been applied successfully to the optical fiber platform, as discussed below.

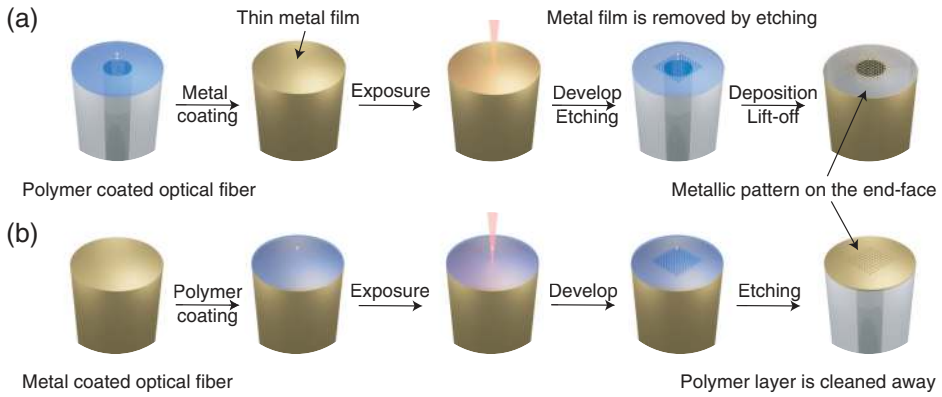

Fig. 6 Schematic illustration of the EBL process to make metallic patterns on optical fibers. (a) A layer of electron beam resist is first coated on the cleaved optical fiber, followed by depositing a thin metal film to improve the conductivity of the fiber. (b) A layer of metal is first deposited on the optical fiber, followed by a coating layer of electron beam resist.

2.2.1 Self-assembly

SA provides a convenient, fast, cheap, and high throughput nanofabrication approach in which the disordered components interact autonomously to form the basic structural units and then spontaneously aggregate into stable structures, resulting in these structures exhibiting certain features that are characteristic of noncovalent bonds (e.g., electrostatic attraction). Because of the abundant hydroxyl groups exposed on the silica surface, the optical fibers can be decorated easily with a silane coupling agent.[114] For example, the chemical decoration using (3-aminopropyl)triethoxysilane [APTES; $NH_2(CH_2)_3$-Si-$(OC_2H_5)_3$] on the optical fiber surface creates abundant amino groups exposed outside, which tend to draw H^+ ions in a solution phase and are positively charged. When immersed in nanomaterial suspensions, the amino groups on the fiber surface attract the negatively charged nanostructures through the electrostatic force. In contrast, chemical decoration using carboxyethyl silanetriol sodium [CEOS; $NaOOC(CH_2)_2$-Si-$(OH)_3$] creates abundant negatively charged carboxyls on the fiber surface that adsorb positively charged nanostructures.

In recent years, several methods have been proposed for patterning optical fiber endfaces using SA.[115,116] For example, Jeong et al. realized an optical fiber localized surface plasmon resonance (LSPR) biosensor by integrating spherical Au nanoparticles (NPs) on the fiber tip. The Au NPs were synthesized using the Turkevich method and then immobilized on the surface of the fiber using SA.[117] Adopting a similar approach, Sciacca and Monro[118] demonstrated the detection of different target analytes on a single optical fiber probe by exploiting different NPs (Au and Ag), on which different antibodies were immobilized. Recently, Liu et al.[119] reported a laser-induced SA method that used the light guided by the optical fiber to assist the arrangement of NP clusters on the fiber endface, thus demonstrating a reproducible optical fiber SERS probe with high sensitivity.

In most cases, the nanostructures produced by SA are often distributed randomly and cannot be controlled precisely. Presented with this problem, Yap et al.[120] demonstrated the template-guided SA of Au NPs into ordered arrays of uniform clusters for high-performance SERS both on flat substrates and optical fiber endfaces. They used spin-coating to fine-tune the template separations by adjusting the spin-coating speed and controlled the distribution of the Au clusters on planar substrates successfully. For optical fiber tips, they used the drop-coating method to make templates, with their attempt to reproduce the same processes on optical fibers leading to close-packed but unordered Au clusters. This cluster ordering issue might be solved using spin-coating to fabricate the template.

In contrast to the SA approaches using NPs, Pisco et al.[121] exploited an SA phenomenon known as breath figure formation to fabricate polymeric honeycomb structures on optical fiber endfaces. The rapid evaporation of a polymer solution results in the condensation of water droplets, which self-assemble into a close hexagonal arrangement at the polymer solution/air interface. After the evaporation of condensed water and residual polymer solvent, a thin metal film was coated on the prepared polymeric honeycomb structure, forming a metal–dielectric PC. Nanosphere lithography has also been widely used to build nanoarray structures, where nanospheres are self-assembled in a hexagonal array on the surface of water. This array of nanospheres can be easily transferred onto an optical fiber endface to form nanoarray structures.[122–124]

2.2.2 CVD/PVD processing

The CVD process is a common bottom-up approach used to grow high quality nanomaterials and nanostructures, such as NPs, nanotubes, nanowires, 2D materials, metal-organic frameworks, as well as other architectures; it is aided by different reaction chambers and growth-enhancing methods. In typical CVD, one or more volatile precursors accumulate and react at the substrate surface to produce the desired deposit. Reactions within the reaction chambers can be achieved either with temperature or with plasma (PECVD). For example, Rabeau et al.[125] used the CVD method to deposit diamond crystals with optically active defects on the optical fiber endfaces, with the fiber capturing the fluorescence generated via the defects in the diamond.

The PVD process is another bottom-up approach deployed to produce thin films and coatings, in which the material transitions from a condensed phase to a vapor phase and then back to a condensed film on the substrate surface. Typical PVD methods include evaporation, sputtering, and epitaxial growth, which are all compatible with the optical fiber platform. For instance, Chen et al.[126] used the magnetron sputtering deposition method to deposit a high-quality WS_2-MoS_2-WS_2 heterostructure based on saturable absorbers onto the optical fiber surface, thus realizing a high-performance all-fiber laser system. Alternatively, Lee et al.[127,128] proposed a high-temperature sensor whereby electron beam evaporation was used to deposit $ZrO_2/Al_2O_3/ZrO_2$ three-layer FP structures on sapphire fiber surfaces.

As mentioned above, the CVD/PVD process can fabricate tailored thin material films and nanostructures on optical fiber surfaces and is further able to handle multiple fibers in one step, which is useful for mass production. Less positively, it is challenging to achieve precise control of the geometrical and physical parameters of the structures.

2.2.3 3D direct laser writing

As a bottom-up 3D direct writing technique, TPL, as in multiphoton lithography (MPL), facilitates the fabrication of arbitrary 3D nanostructures with sub-100 nm features.[129,130] A typical TPL direct writing system consists of a laser that provides strong near-infrared fs laser pulses, suitable photoresist materials, a precise 3D nanoposition stage, and a computer that controls the writing process. The focused fs laser has extremely short pulse duration and extremely high peak power at the focal point, which transfers energy to the material via a nonlinear process in a short period of time. In TPL, the fs laser is focused intensely on the photosensitive resist to induce two-photon absorption, which instigates polymerization of the photoresist at the focal point. The laser intensity at other locations on the optical path is not sufficient to induce two-photon absorption, while the energy of a single-photon is not sufficient for photopolymerization to occur. Thus, via precise 3D scanning of the focal laser spot using a computer, the polymerized resist exhibits the desired 3D arrangement with an impressive spatial resolution.

More recently, microphotonic structures featuring different TPL-generated shapes and structures on optical fiber endfaces have been widely reported (see Fig. 7).[134–141] For example, Williams et al.[131] used multiphoton direct laser writing to fabricate various components, including refractive lenses and 3D woodpile PCs, within the resin on the endface of the optical fibers. Similarly, Gissibl et al.[132,142] presented free-form micro-optical elements, including spherical lenses, toric lenses, chiral

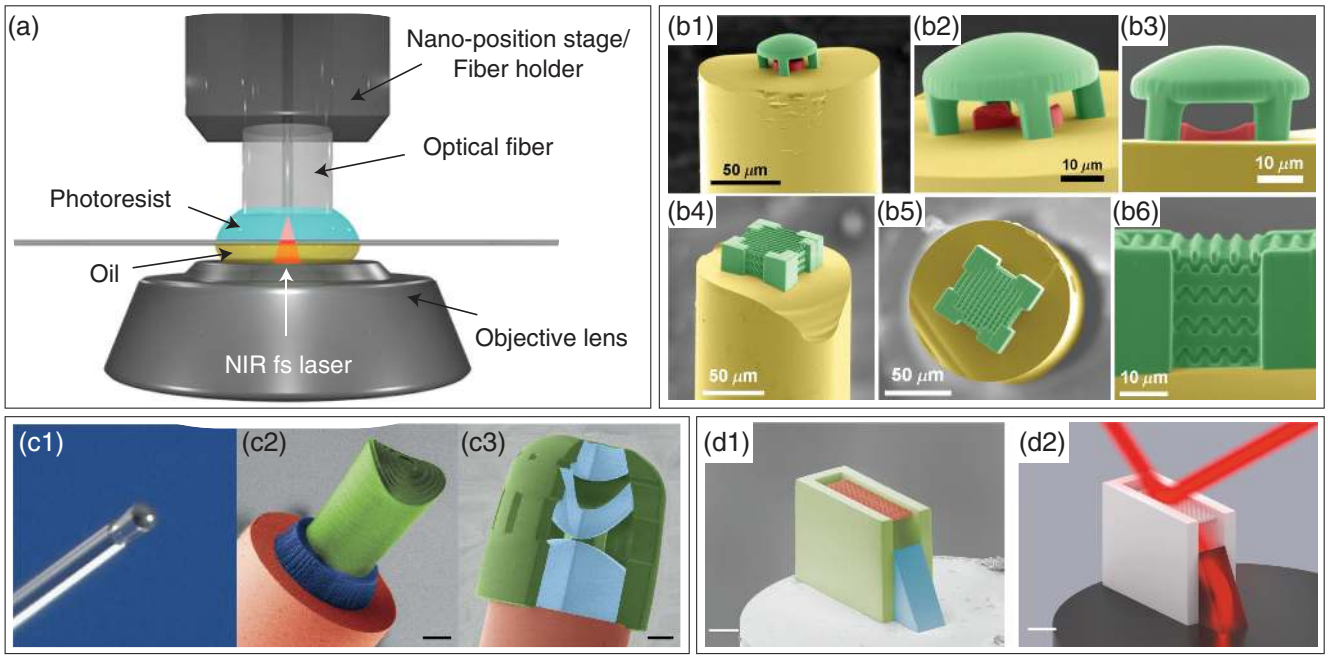

Fig. 7 3D direct laser writing technique based on TPL/MPL. (a) Schematic illustration of the TPL/MPL fabrication system, including an optical fiber fixed in fiber holders, a photoresist, a glass slide, optical matching oil, and an objective lens. (b1)–(b3) False-color SEM images of a compound microlens system on a fiber endface. (b4)–(b6) False-color SEM images of a woodpile face-centered tetragonal PC created on a fiber endface.[131] Copyright 2011, Optical Society of America. (c1)–(c3) Different functional optical elements integrated on fiber tips. The scale bars are 25 μm.[132] Copyright 2016, Springer Nature. (d1), (d2) False-color SEM image and the rendered view of a polarizing beam splitter on a fiber endface. The scale bars are 10 μm.[133] Copyright 2018, Optical Society of America.

PC structures, and multilens objectives, integrated on optical fiber endfaces with submicrometer accuracy for numerous applications involving beam shaping, collimation, focusing, and imaging. Benefiting from the high degree of control and processing freedom afforded by TPL, Xie et al.[143,144] demonstrated a 3D SERS radar on optical fiber endfaces using a series of 3D direct writing techniques, such as thermal evaporation and UV laser pulse irradiation. Furthermore, Kim et al.[145] fabricated a range of SERS arrays on both planar substrates and optical fiber endfaces with strong repeatability and consistency, highlighting the suitability of this technique for mass production. More recently, Zhang et al.[146,147] demonstrated a 3D optical microsystem on the endface of a multicore optical fiber, enabling the excitation and detection of whispering gallery modes, which can be used for sensing volatile organic compounds (VOCs).

In addition, a 3D microprinting technology was reported by Yao et al.[148–151], using a UV grade DMD and a 365-nm UV source to fabricate SU-8 based ferrule-top suspended-mirror devices on fiber endfaces.

2.2.4 Self-guiding photopolymerization

Self-guiding photopolymerization is a unique bottom-up method for fabricating micro-optical structures on optical fiber endfaces, which uses the guided light emerging from the fiber core to modify external photopolymerizable materials. After exposure and rinsing, a polymer tip is bonded firmly to the fiber as an extension of the fiber core.[152] The geometry of the polymer tip can be controlled via optical and physicochemical parameters, such as laser intensity, exposure time, oxygen quenching, and internal filtering.[153] The fabricated polymer tip can reach hundreds of microns in length by dipping a single-mode fiber into a thick layer of photopolymerizable solution.[154,155] When the photopolymerization process is applied to a multimode fiber, a 3D polymer mold of the fiber's linearly polarized modes can be obtained, which is controlled by the coupling of the incident light beam to the optical fiber. These prepared polymer tips have been used for coupling light from single-mode optical fibers to small core photonic-crystal fibers (PCFs) and subwavelength single-mode silicon-on-insulator (SOI) waveguides.[156,157] Moreover, optical tweezers were also realized using two polymer tips to construct a counterpropagating optical trap.[158]

2.3 Material Transfer Methodologies

In addition to the aforementioned methods, which are all processed directly on the tips of the optical fibers, material transfer methods have been developed extensively as indirect fabrication approaches. These methods are based on transferring prefabricated nanostructures and nanomaterials from planar substrates to fiber endfaces, thus benefiting from the well-developed nanofabrication techniques available for the planar platform. Several transfer methods have been proposed, each striving to ensure the structural integrity and improve the fabrication yield. In the following sections, the material transfer methods were divided into two parts; namely, methods involving the direct transfer of the

nanomaterial and those involving the nanotransfer of nanostructures.

2.3.1 Direct transfer

To date, numerous nanomaterials, including quantum dots, nanowires, and nanotubes, and 2D materials have been transferred directly to optical fiber endfaces through van der Waals interactions. Different direct transfer methods are associated with different nanomaterials dispersion systems, such as the dip-coating method for transferring nanomaterials from solutions or suspensions,[159] the wet-transfer method for transferring 2D materials from a water surface,[160] and the micromanipulation method for precise transferal when forming heterostructures.[36]

In recent decades, passively Q-switched and mode-locked fiber lasers have been fabricated using the direct transfer of materials or materials-polymer composites, with these materials serving as saturable absorbers, to the optical fiber endfaces.[161–163] Similarly, all-in-fiber photodetectors (FPDs) have also been proposed based on a pair of endface electrodes bonded with few-layer molybdenum disulfide (MoS_2) or $CsPbBr_3$–graphene hybrid structures.[38,164] The interaction forces between the optical fiber endfaces and the transferred materials (especially some hard films) are weak, leading to the unreliable performance of the fiber devices. To overcome this unreliability, Calero et al.[165] employed the point welding method to immobilize a film of lithium niobite ($LiNbO_3$) on a fiber endface.

Although the direct transfer methods discussed above can fix a large area of nanomaterials on the fiber endfaces, it is challenging to control the size and shape of the materials accurately. In response, Xiong et al.[36] integrated a graphene-MoS_2-WS_2 heterostructure film with the electrodes on the optical fiber endface via a simple layer-by-layer micromanipulation transferal method, as shown in Fig. 8. This transfer method is a flexible, precise, and low-cost approach that can also be used to transfer nanostructures preprepared on a planar substrate to optical fiber endfaces as well as other substrates. However, the complicated fabrication process results in a low yield, which impedes mass production using this approach.

2.3.2 Nanotransfer

Nanotransfer methods are based on transferring prefabricated nanostructures from planar substrates to the fiber tips, thus benefiting from the well-developed nanofabrication techniques available for the planar platform. According to the sequences of the transfer process, proposed nanotransfer approaches can be categorized as either "release and attach" or "contact and separate."[23]

In the "release and attach" approach, the nanostructures on the planar substrates are first detached from the substrates and then transferred onto the fiber endface. Smythe et al.[166,167] initially demonstrated a "decal transfer" method to transfer metallic nanostructures from silicon substrates to the optical fiber endfaces. In this case, Au patterns were first fabricated on silicon substrates using standard nanofabrication techniques before being stripped off by a composite polymer comprising polydimethylsiloxane (PDMS) and a thin film of sacrificial thiolene. Then, the optical fiber was aligned and pressed onto the polymer film, resulting in the release of the thin thiolene film along with the Au patterns, which were adhered to the fiber endface by van der Waals forces. After removing the sacrificial thiolene film, optical fiber-based SERS probes with periodic Au arrays were realized. The most difficult aspect of this approach is to compare and adjust the interaction forces between the substrates, the polymers, and the patterns to ensure the success of the step-by-step transferal. To simplify the process, Whitesides et al. conceived a transfer process using the nanoskiving technique and the wet-transfer method. In the nanoskiving process, epoxy nanostructures were prepared by soft-lithography and then coated with thin metallic films, before being embedded in epoxy and, finally, sectioned into slabs by an ultramicrotome. The membranes floated on the water's surface and were transferred to the optical fiber endfaces by wet-transfer. The metallic

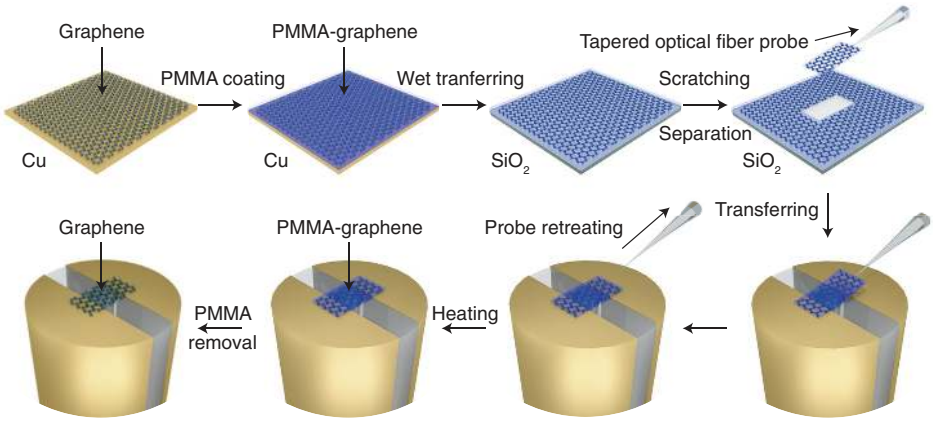

Fig. 8 Schematic illustration of the micromanipulation method to transfer 2D materials onto the optical fiber electrodes to fabricate photodetectors, taking graphene as an example.[36] First, a PMMA film is spin-coated on the graphene. After removing the original substrate, the PMMA-graphene composite film is transferred to a glass slide via the wet-transfer method. A tapered optical fiber is used to scratch and separate a certain shape of the PMMA-graphene film and transfer it onto the electrodes on the optical fiber endface. Then, the fiber is heated to improve the contact between the composite film and the fiber endface. Finally, the PMMA is removed, and the graphene layer is bonded strongly to the fiber glass and the metal electrodes.

nanostructures on the fiber endface were obtained after the removal of the epoxy by PE.[168] In contrast to discrete nanoarrays, large-sized structures such as PCs can be transferred directly using a micromanipulation method. For example, Jung et al.[169] successfully transferred a PC slab to the fiber endface using an FIB tool fitted with a micromanipulator. Similarly, Wang et al.[170] released a PC nanocavity membrane from its original substrate and attached it to the fiber endface via micromanipulation using a tapered fiber. This type of process requires high flatness of both the optical fiber endfaces and the nanostructured membranes so that sufficient van der Waals forces are obtained to bond the nanofeatures.

For the "contact and separate" approach, the optical fiber endfaces are first coated with an adhesion layer such as an epoxy or ultraviolet (UV) curable resist and then aligned and placed into contact with the nanostructures on planar substrates. After the subsequent curing of the adhesion layer, the nanostructures are separated from the original substrate and bonded strongly to the fiber endfaces.[171] Thus, Shambat et al. demonstrated a simple and rapid epoxy-based method for transferring PC cavities to optical fiber endfaces. In this case, the optical fiber cladding area was first coated with a layer of epoxy by a sharp electrical probe on a micromanipulator stage. After the optical fiber was aligned and contacted to the PC structure, it was released gradually as the epoxy cures, with the PC structure adhering to the fiber endface.[172,173] The micromanipulation method used here can prevent contamination of the optical fiber core and protect the central PC cavities. To simplify the approach, Jia and Yang[174–177] transferred nanohole and nanoslit arrays from Au-coated templates to optical fiber endfaces by means of depositing epoxy layers on the entirety of the fiber endfaces.

As with epoxy, UV glue is a popular medium used to separate and transfer nanostructures to optical fibers, with this method operating similarly to the NIL process to a certain extent.[178] For example, Lin et al. demonstrated the fabrication of plasmonic fiber probes via a UV glue-based structure transferal method. After a spherical packed polystyrene (PS) template had been prepared, the PS spheres were embedded in a thin UV glue layer precoated on the fiber endface and subsequently removed to construct the closely arranged nanocavities.[179] With the help of UV glue, Arce et al. successfully integrated an SOI photonics sensor on an optical fiber endface. Notably, a layer of wax was coated between the substrate and the structure, serving as a sacrificial layer to facilitate the separate processes.[180]

3 Structures and Applications

The previous section introduced numerous studies in which the integration of micro- and nanostructures onto the flat tips of optical fibers has been proposed. Optical fiber devices possess many advantages, such as small size, light weight, electromagnetic immunity, and remote sensing capability. Herein, we review the typical structures encountered on fiber tips and their known and potential applications, which we have categorized with respect to functional structure configuration, including the optical functionalization of optical fibers and electrical integration on optical fibers (Fig. 9).

3.1 Optical Functionalization

In recent decades, various optical structures have been fabricated on optical fiber tips successfully, covering diverse applications in the fields of beam-shaping, collimation, focusing, signal processing, imaging, sensing, and particle trapping among others. Considering that the optical structures integrated on the fiber tips have different sizes, shapes, dimensions, and light–matter interaction approaches, they can be classified into two categories, those belonging to 3D miniature structures and those belonging to 2D functional surfaces.

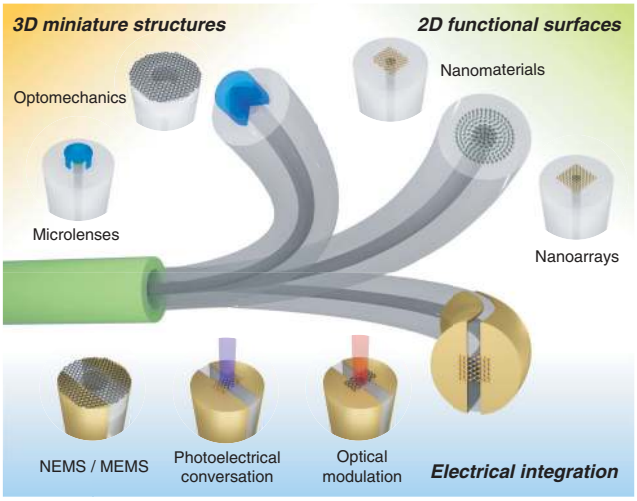

Fig. 9 The paradigm of multifunctional structures integrated on optical fiber tips. The fiber tip devices were classified with respect to functional structure configuration, including (top left) the 3D miniature micro-optics structures, (top right) 2D textured nano-optics surfaces, and (bottom) electrodes integrated on fiber tips.

3.1.1 3D miniature structures

The diversity of applications and the requirements of compact optical systems have driven the development of 3D miniature optical elements on the order of the fiber diameter. As discussed in the previous section, a variety of fabrication techniques have been developed to integrate minimized optical components onto optical fiber tips, including FIB, fs laser ablation, chemical etching, and two-photon direct laser writing. The following short sections review the typical minimized 3D miniature optical structures integrated on fiber tips, which include optomechanical structures and micro-lenses.

Optomechanics. Fiber-optic optomechanics refers to the technologies concerning the design and manufacture of micron-scale optomechanical structures on optical fibers. Typical optomechanical structures include cantilevers and suspended membranes forming FP cavities.

Sensing. FP resonance cavities built on optical fiber tips have been studied extensively to produce sensors for pressure, temperature, vibration, and acoustics in remote, space limited, and harsh environments. An FP cavity consists of two or more parallel reflecting mirrors, in which interference arises due to the superposition of both reflected and transmitted beams between the two parallel surfaces. Typical fiber-optic FP interferometers consist of an optical fiber-cavity-thin film structure, in which capillaries, coreless fibers, hollow fibers, certain fiber fusion structures (e.g., bubbles), and certain smart materials (such as microgels) are used to form resonant cavities covered with thin films such as silica films, metal films, and 2D materials films.[44–48,50,181–183]

Imaging. Iannuzzi et al.[70,71,184] fabricated cantilever structures on fiber-tops by utilizing FIB and fs laser micromachining applied for contact mode AFM imaging. In addition, polymer-capped optical fiber tips were also investigated as FP interferometers, with applications including ultrasound sensors, photoacoustic transducers, and 3D endoscopy.[185–189] For example, Guggenheim et al.[190] proposed an optical fiber probe for ultrasound detection based on a planoconcave polymer microresonator with strong optical confinement (Q-factor $> 10^5$), which showed high ultrasound sensitivity with an excellent broadband acoustic frequency response and wide directivity. On the other hand, for ultrasound excitation, multiwalled carbon nanotube (MWCNT)-PDMS composites are a typical material used for photoacoustic transducers.[191,192] Using this approach, Finlay et al. reported an all-optical ultrasound transducer consisting of two optical fibers that can generate and receive ultrasounds, respectively, and it was applied to real-time invasive medical imaging *in vivo*. The ultrasound was generated through the photoacoustic excitation of MWCNT-PDMS on the fiber endface via a pulsed laser, with the returning ultrasound signal detected by a high-finesse FP cavity on a single-mode optical fiber. A custom-built inner transseptal needle with a metallic septum was used to encapsulate and isolate the two optical fibers, which was then used within the beating heart of a pig to provide real-time views of the cardiac tissue.[193] Other than the above examples that used a single fiber for excitation or reception of an ultrasound, Ansari et al. demonstrated a miniature forward-viewing 3D endoscopic probe, which consisted of a coherent optical fiber bundle with a mirror-polymer-mirror FP ultrasound sensor at its endfaces. The sensor comprised 50,000 individual elements within the 3.2-mm outer diameter of the probe, affording fine spatial sampling and high-resolution photoacoustic images.[187]

Moreover, in order to identify specific substances accurately, FP interferometers built at optical fiber tips can be integrated with multiple kinds of nanomaterials, thus combining the characteristics of the nanomaterials and the features of FP cavities, which will be discussed further in Sec. 3.1.2. Optical fiber-based MEMS/NEMS devices were also investigated, which will be discussed in Sec. 3.2.1.

Microlenses. Lens systems are an integral component of applications involving beam-shaping, collimation, focusing, and coupling and are frequently subject to restrictions relating to their size, shape, and dimensions, owing to the limitations of lens fabrication techniques. Microlenses are miniaturized lenses, typically involving parameters on the micrometer scale. In recent decades, microlenses with various lens designs have been integrated successfully onto optical fiber tips. This has been realized for lens designs including planoconvex-lenses, biconvex-lenses, spherical lenses, toric lenses, and multilens composite structures, to name just a few (Fig. 10).[132] The integration of small high-performance microlenses onto optical fibers requires submicrometer alignment accuracy relative to the fiber core, making it difficult to transfer the microlenses to the fiber tip precisely. Therefore, most microlenses are processed directly on the fiber endface using methods such as FIB milling, chemical etching, 3D direct laser writing, and NIL.[56,59,69,133,136,139,194–198] As an example, Gissibl et al.[142] demonstrated the complete process chain for high-performance multilens objectives on fiber endfaces with sizes of ~100 μm, indicating its potential application in the fields of beam shaping, endoscopy, illumination, imaging, inspection, and microscopy on the micrometer scale. The same research team proposed submicrometer dielectric phase masks on single-mode optical fiber endfaces for spatial beam intensity shaping [Fig. 10(a)].[140] Moreover, optical tweezers have been proposed that involve the fabrication of microstructured optical fiber endfaces, which are created using FIB milling.[68,72]

3.1.2 2D functional surfaces

The continuous development of nanoscience and nanotechnology makes addressing the feasibility of optics on the nanometer scale inevitable. As mentioned above, a variety of fabrication techniques have been explored to create nano-optical structures directly on optical fiber endfaces, such as FIB milling, EBL, NIL, and SA. In contrast to micro-optical devices, nanostructures with discrete 2D planar nanofeatures can be transferred easily to the surface of optical-fiber endfaces, using the so-called nanotransfer method. To date, several typical nano-optical structures have been integrated on fiber endfaces successfully, such as nanomaterials, periodic nanoarrays, and metamaterials, which will be discussed in the following sections.

Nanomaterials integration. The useful properties of nanomaterials and the features of optical fibers can be combined to produce an attractive platform for various applications, such as lasing and sensing.

Lasing. Pulsed fiber lasers have been applied in fields ranging from optical frequency metrology to nonlinear wavelength conversion and from nonlinear microscopy to investigating the dynamic evolution of solitons.[199–202] Set et al.[163] presented the first passively mode-locked fiber lasers based on a carbon nanotube (CNT) saturable absorber. Since then, passively Q-switched and mode-locked fiber lasers have been integrated on optical fiber endfaces using various saturable absorbing nanomaterials, including NPs, CNTs, graphene, topological insulators (e.g., Bi_2Te_3, Bi_2Se_3, Sb_2Te_3), transition metal dichalcogenides, black phosphorus, and material composites.[126,160–162,203–213] Taking graphene as an example, the interband optical absorption in zero-gap graphene can be easily saturated under strong excitation due to Pauli blocking. Following this principle, Bao et al.[160] demonstrated a mode-locked fiber laser for the generation of ultrashort soliton pulses within the telecommunications band, using atomic layer graphene as a saturable absorber.

Chemosensing. Further, nanomaterials including metals, metal oxides, their composites, as well as low-dimensional materials such as CNT, graphene, and graphene oxides have been implemented for fiber-optic physical, chemical, and biological sensors.[15,117,118,127,128,159,214–225] Incorporating the principles of Fresnel reflection, interferometers, and surface plasmon resonance (SPR), respectively, various nanomaterial films have been integrated onto fiber tips, thus demonstrating chemical sensors tailored to the detection of specific gases, VOCs, and heavy metal ions.[15,214,226] Predominantly, these fiber-based sensors exploit the sensing characteristics of the nanomaterials, which eventually affect the optical structure of the optical fiber sensing system.

Within the last decade, toxic gases (e.g., NH_3, H_2S, NO_2, CO_2) and flammable gases (e.g., CH_4, H_2) have been monitored using these optical fiber-based chemical sensors that comprise sensitive nanomaterial films on fiber tips.[215–224] For example, nanofilms of graphene oxide (GO)-based nanohybrids and porous graphene, as well as Fe_3O_4-graphene composite-coated optical fiber tips, have been investigated for the detection of ammonia (NH_3) at room temperature.[222,223,227] Elsewhere, ZnO NPs

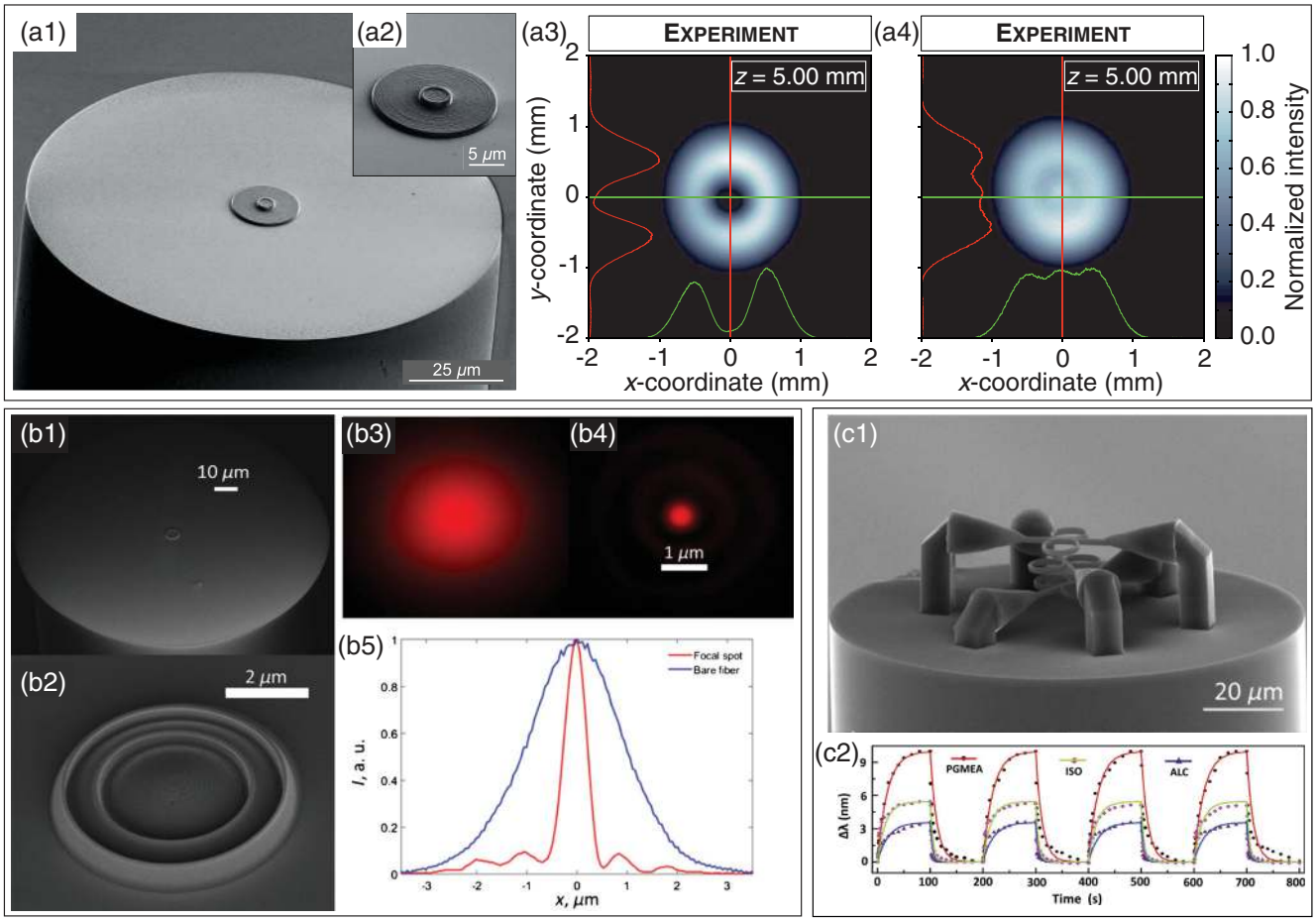

Fig. 10 Micro-optical elements integrated on optical fiber tips. (a) Phase masks on fiber endfaces for spatial beam intensity shaping. (a1), (a2) SEM images of a diffractive optical element on an optical fiber endface. (a3), (a4) Measured intensity distributions for (a3) the doughnut-shaped and (a4) top-hat-shaped diffractive optical elements.[140] Copyright 2016, Optical Society of America. (b) High RI Fresnel lens on a fiber endface for efficient light focusing. (b1), (b2) SEM images of the Fresnel lens on a fiber. (b3), (b4) Light intensity distributions of (b3) a bare single-mode fiber and (b4) a fiber with Fresnel lens. (b5) The corresponding intensity profiles of the light intensity distributions.[194] Copyright 2016, Optical Society of America. (c) Suspended polymer microrings on a multicore fiber endface for multiple gas sensing. (c1) SEM image of the optical tentacle on the fiber endface. (c2) Cycle tests for the sensing reversibility of the optical tentacle in three types of vapor.[147] Copyright 2020, Optical Society of America.

have been embedded into a poly-methyl-methacrylate (PMMA) matrix and coated on the fiber tip for sensing H_2S (at concentrations ranging from 1 to 5 ppm) at room temperature.[221] Furthermore, a lutetium bisphthalocyanine ($LuPc_2$) dispersed mesostructured silica film has been coated on a fiber tip, which was sensitive to NO_2 in the ppm range.[224] Sensitive layers of Pd, Pd-Y, Pt-WO_3, Pd capped alloys, and nanostructured α-MoO_3 [Fig. 11(a)] have been coated both on fiber endfaces and fiber resonance structures, creating high sensitivity hydrogen sensors.[215–218,220,228,229]

Similarly, VOC optical fiber sensors have been demonstrated. For example, a zeolite thin film-coated spherical optical fiber FP cavity was investigated for sensing isopropanol, formaldehyde, and their mixtures by monitoring the wavelength shift of FP interference, which was induced in response to the molecules of the VOCs being adsorbed onto the zeolite film.[230] Alternatively, a nanopatterned GO-TiO_2 film was fabricated on fiber tips to produce a guided mode resonance structure. The structure was able to detect ethylene and methanol vapors with sensitivities of 0.92 and 1.37 pm/ppm, respectively.[231] Elsewhere, optical fiber VOC sensors based on porous silica xerogels have been reported using the sol–gel process, with the resulting sensors showing sensitivity toward dichloromethane, acetone, and cyclohexane.[232]

Beyond sensing gas molecules, various nanomaterial decorated fiber-optic sensors have been explored in relation to heavy metal ion (e.g., Hg^{2+}, Mg^{2+}, Pb^{2+}, Cd^{2+}) detection in liquid solutions. For instance, by immobilizing the organic fluorophore Rhod-5N on the fiber tip, fluorescent sensors for the detection of mercury ions (Hg^{2+}) with a limit as low as 0.3 ppb in aqueous solution have been developed.[233]

Biosensing. Metallic NPs have been fabricated and transferred to fiber tips for biosensing. For example, an LSPR sensor has been fabricated using spherical Au NPs on an optical fiber tip,

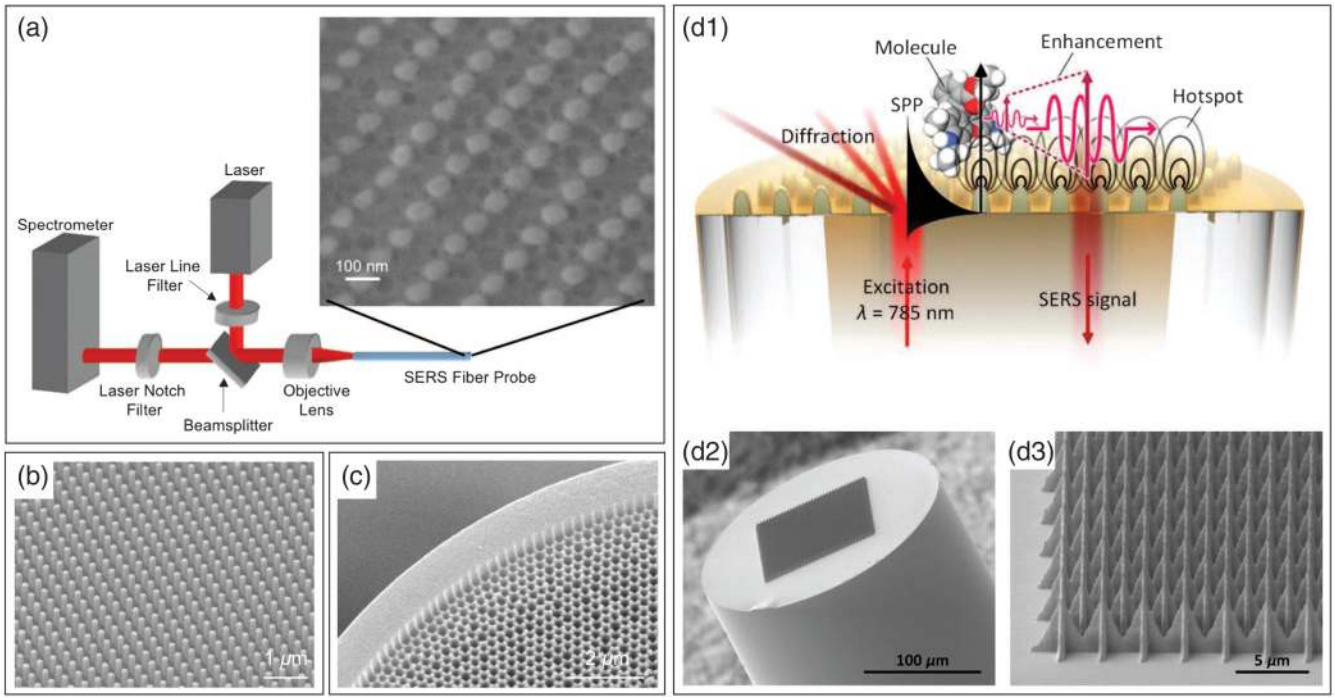

Fig. 11 Optical fiber-based SERS probes. (a) Schematic depiction of the measurement setup for characterizing an SERS probe. Inset: SEM image of an array of Au optical antennas on a fiber endface.[166] Copyright 2009, American Chemical Society. (b) SEM image of the Ag-coated nanopillar array on a fiber endface used for SERS.[96] Copyright 2012, Optical Society of America. (c) SEM image of nanoscale honeycomb structures on a fiber endface for SERS.[66] Copyright 2005, Optical Society of America. (d) SERS-on-a-tip probes based on a nanoarray on an optical fiber endface.[145] (d1) Schematic illustration of the mechanism for Raman scattering enhancement. (d2), (d3) SEM image of the cross-spike array on an optical fiber tip. Copyright 2020, WILEY-VCH Verlag GmbH & Co. KGaA, Weinheim.

which was applied for the detection of antibody–antigen reactions with a detection limit of ~2 pg/mL.[117] Recently, as shown in Fig. 11(b), Sciacca and Monro[118] exploited different metallic NPs (Au and Ag), which have distinct LSPR signatures with limited overlap, achieving multiplexed biosensing on a single optical fiber probe.

Several studies have proposed optical fiber-based SERS probes produced by depositing metallic NPs onto the fiber tips.[119,234–237] Recently, a double-substrate "sandwich" structure was proposed for fiber SERS detection. First, Ag NPs were fabricated using the fiber surface as the SERS substrate, and then the fiber probe was immersed in a solution containing a mixture of Ag NPs and target analyte molecules. The Ag NP structures on the fiber and in the solution randomly sandwich the analyte molecules in between, which enhances the electromagnetic field and thus produces the SERS signal. By exploiting this principle, the highly sensitive detection of R6G, proteins lysozyme and cytochrome c has been demonstrated [Fig. 11(c)].[159,235]

Notably, a variety of approaches for fiber-optic sensing applications have been explored on side-polished D-shaped fibers, unclad fibers, tapered fibers, and fiber Bragg gratings, benefiting from the long matter–environment interaction distance.[15,23,114,238,239]

Imaging. Nanomaterials-coated fiber endfaces can be regarded as multiple-scattering tips for imaging applications such as microendoscopy. Shin et al. demonstrated 2D single-pixel imaging using illumination via a TiO_2-coated single-mode fiber and compressed sensing acquisition. The TiO_2-coated fiber endface was a multiple-scattering surface that produced randomly structured, but deterministic, speckle patterns to illuminate the target object. Using a single photodetector to collect the scattered light, the images of the object can be reconstructed from the wavelength dependence of the speckle patterns and the total light of the object.[240]

Nanoarrays integration. As discussed in Sec. 2, metallic nanoarrays with various nanofeatures have been fabricated on fiber endfaces, including periodic, quasiperiodic, or random distributions of nanopillars, nanodots, nanoholes, nanodisks, and nanogratings. These devices have been demonstrated in applications in numerous fields, including chemical and biological sensing, beam operations, nonlinear photonics, and optical tweezers. It is notable that, metasurfaces (MSs), as 2D artificial electromagnetic media on the subwavelength scale, can guide and control the propagation of electromagnetic waves by engaging resonance excitations such as localized plasmonic modes.[241–243] The integration of MSs and optical fiber technologies facilitates the control of light using nanoscale arrays on the fiber endface, which can be applied in the fields of communications, signal processing, imaging, as well as sensing.

Sensing. Light–matter interaction occurring in subwavelength metallic nanostructures can be enhanced by several orders of

magnitude via LSPR. Therefore, every alteration at the sensor surface, such as changing the RI, temperature, or the binding of molecules, results in the resonant wavelength(s) shifting. According to this principle, numerous optical fiber-based RI sensors for the quantitative analysis of chemical reactions and biological interactions have been demonstrated, based on arrays of metallic nanodisks,[87] nanodots,[86,113] nanoholes,[76,77,175,176,244–246] nanoslits and nanogratings,[95,174,247–249] nanopillars and nanorods,[250,251] nanorings,[89] nanotrimers,[252] and metal–dielectric nanocrystals.[88,112,121] For example, Jia et al.[174] constructed plasmonic optical fibers by transferring patterned metal nanostructures onto optical fiber endfaces, which showed narrow linewidths (6.6 nm) and a high figure of merit (60.7). The plasmonic fiber probe was first characterized as an RI sensor using different concentrations of NaCl solution with a transmission sensitivity of 595 nm per refractive index unit. Then, the probe performed label-free and real-time biosensing using the immunoassay of the antigen–antibody, revealing a detection limit of 8.5 pg mm^{-2}. Recently, Aliberti et al.[253–255] integrated microgels onto a plasmonic nanohole array prefabricated on a fiber endface, which concentrated the target molecule and thus enhanced the optical response.

Other than via the LSPR principle, nanostructures integrated on fiber endfaces have been applied as chemo- and biosensors based on SERS. In general, the SERS effect can lead to a millionfold enhancement of the Raman scattering intensity for molecules, which is attributed to either the electromagnetic enhancement or the chemical interaction between the SERS active surface and the attached target molecules. In recent decades, optical fiber-based SERS probes have been exploited by integrating various kinds of nanoarrays, including periodic arrays of nanoscale optical antennas [Fig. 11(a)],[166] nanorods and nanopillars [Fig. 11(b)],[96] nanoholes,[73] nanocavities,[179] and honeycombs [Fig. 11(c)],[66] as well as randomly distributed arrays of nanorods,[256] NP clusters,[120] and replicas of nanotemplates.[102,109] Recently, as shown in Fig. 11(d), Kim et al.[145] used two-photon polymerization and subsequent metallization to fabricate three types of nanoarrays on the endfaces of optical fibers, presenting a fiber-optic SERS probe for the rapid detection of bacteria. The probes showed a detection limit of R6G of 10^{-7} mol/L, while the enhancement factor was measured as 1300, which was then applied for rapid SERS detection of live *Escherichia coli* cells with Raman integration time ranging from milliseconds to seconds. Consales et al.[257] used phase-gradient plasmonic MS on the optical fiber tip to detect biomolecular interactions with a limit of detection of the order of a few ng mL^{-1}.

Beam shaping and operation. In addition to the nanostructures mentioned above, metallic nanogratings on optical fiber endfaces exhibit unique optical properties due to the surface plasmon polaritons that result from the light confined in optical fibers interacting with the subwavelength nanograting. These nanogratings can be utilized as optical filters,[258,259] amplifiers,[258] polarizers,[85] beam splitters,[107] and metallic Fresnel zone plates,[260] as well as in applications requiring waveguide coupling,[106] Bessel beam generation,[74] wavelength-division-multiplexing signal monitoring,[81] and wavelength-dependent off-axis directional beaming.[261] In addition to that, meta-fiber tips are also widely demonstrated for beam shaping and operation. For example, Principe et al.[78] proposed a phase-gradient plasmonic MS integrated on a fiber tip [Fig. 12(a)], enabling an impinging beam to be guided in desired directions. A 50-nm Au layer with different rectangular nanoholes was patterned in the plane of the fiber endface. By tuning the nanohole sizes appropriately to correspond to the resonance frequency, an arbitrary phase (within the full 2π range) can be induced in the transmitted/reflected components with suitable polarization. Specifically, interactions between ordinary and anomalous beams can be realized by adjusting the angles of the prototype according to the array-induced phase-matching mechanism. This MT configuration was applied for beam polarization and phase gradient control.[262] Similarly, Yang et al.[263] reported an optical metalens patterned on the core area of a PCF endface to be used for light

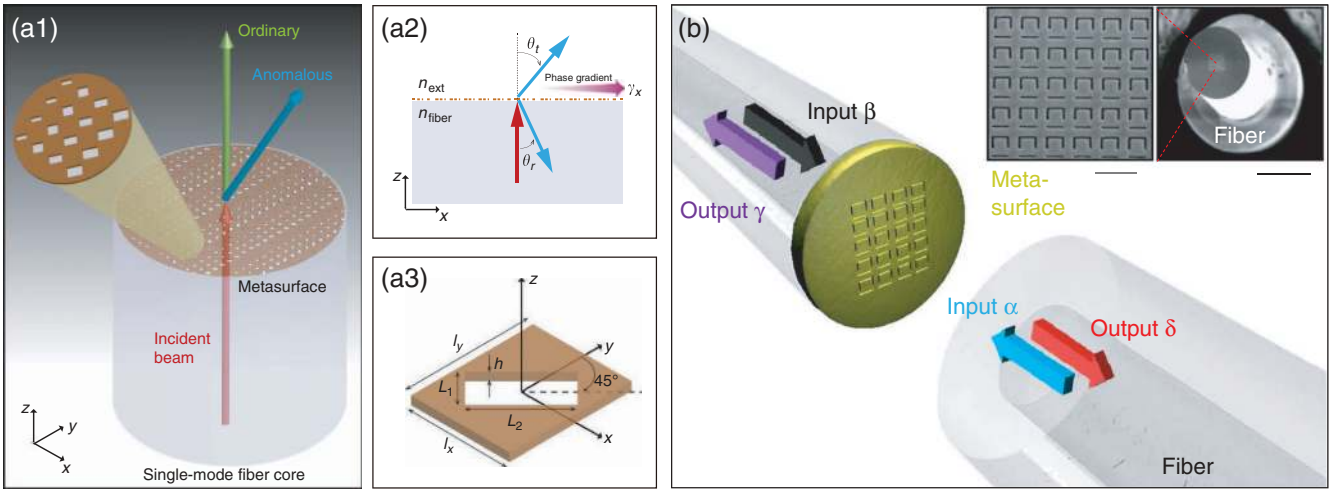

Fig. 12 Metasurfaces on optical fiber tips. (a) An optical fiber MT for beam steering and coupling. (a1) Schematic view of the MT with a plasmonic MS fabricated on the endface. (a2) Illustration of the MT operating principle. (a3) Geometry of the rectangular nanoaperture realized in an Au layer.[78] Copyright 2016, Springer Nature. (b) Schematic illustration of an MS-covered optical fiber tip for all-optical signal modulation based on coherent absorption. The insets are SEM images of the device, black scale bar: 100 μm, gray scale bar: 1 μm. Copyright 2018, Springer Nature.

focusing at communications wavelengths, which showed a maximum enhanced optical intensity as large as 234% at the focal point of the lens. Moreover, Xomalis et al.[264] reported a fully fiberized and packaged optical switching meta-fiber device based on coherently controlled absorption [Fig. 12(b)]. Within a coherent fiber network, logical functions of XOR, NOT, and AND were performed at wavelengths between 1530 and 1565 nm, indicating potential in the field of coherent and quantum information networks.

Optical tweezers. Optical tweezers have been instrumental for manipulating micro- and NPs accurately and noninvasively. Conventional optical tweezers are used typically to trap and manipulate micron-scale objects, while they are incapable of trapping nanoscale objects directly. This is because trapping NPs requires an ultrahigh optical power to increase the optical forces, which leads to photothermal issues. Moreover, owing to the diffraction limit, the size of the optical trap is often hundreds of times greater than the size of NPs. To overcome the weak optical forces and photothermal issues accompanying conventional optical tweezers, plasmonic optical tweezers, which have strong field gradients that can trap and manipulate NPs with lower optical power levels, have been developed.[265–269] Recently, plasmonic optical tweezers have been integrated on the endfaces of optical fibers, enabling the 3D manipulation of trapped nanoscale particles.[270] In pioneering work proposed by Berthelot et al.,[271] a bowtie-shaped plasmonic aperture was fabricated at the endface of a tapered Au-coated optical fiber, demonstrating near-field nanotweezers for 3D optical trapping, manipulation, and trapping status monitoring of individual 50-nm dielectric particles. The trapped objects were able to be moved over distances measuring tens of micrometers in several minutes using very low in-trap intensities. Similarly, Gelfand et al.[272] built a double nanohole aperture on an Au-coated endface of a nontapered optical fiber, demonstrating the trapping and monitoring of individual 20- and 40-nm diameter PS spheres (Fig. 13). To improve the mode matching and optical coupling of the plasmonic structure, Saleh et al.[273] designed a fiber optic plasmonic tweezer with subwavelength coaxial geometry, which was fabricated on a fiber endface and can trap sub-10-nm dielectric particles.

Imaging. In the field of imaging, optical aberrations and the trade-off between transverse resolution and depth of focus are technological challenges. Pahlevaninezhad et al.[274] integrated a metalens into a fiber-based nano-optic endoscope to modify the phase of incident light at the subwavelength level, realizing near diffraction-limited imaging by negating nonchromatic aberrations.

3.2 Electrical Integration

Owing to the limitations of the material characteristics of optical fibers (most often SiO_2), they do not possess electronic and optoelectronic functions, which limits their application. In the 2000s, researchers tried to integrate different materials and microstructures into optical fiber configurations while drawing the fiber, making fibers that can see, hear, sense, and communicate.[1–12] This field of "multimaterial fibers" arouses great industrial interest but also faces some technological challenges. In this section, we discuss several recently proposed device designs for electrical integration on optical fiber endfaces, which use commercially available standard optical fibers and simpler fabrication methods.

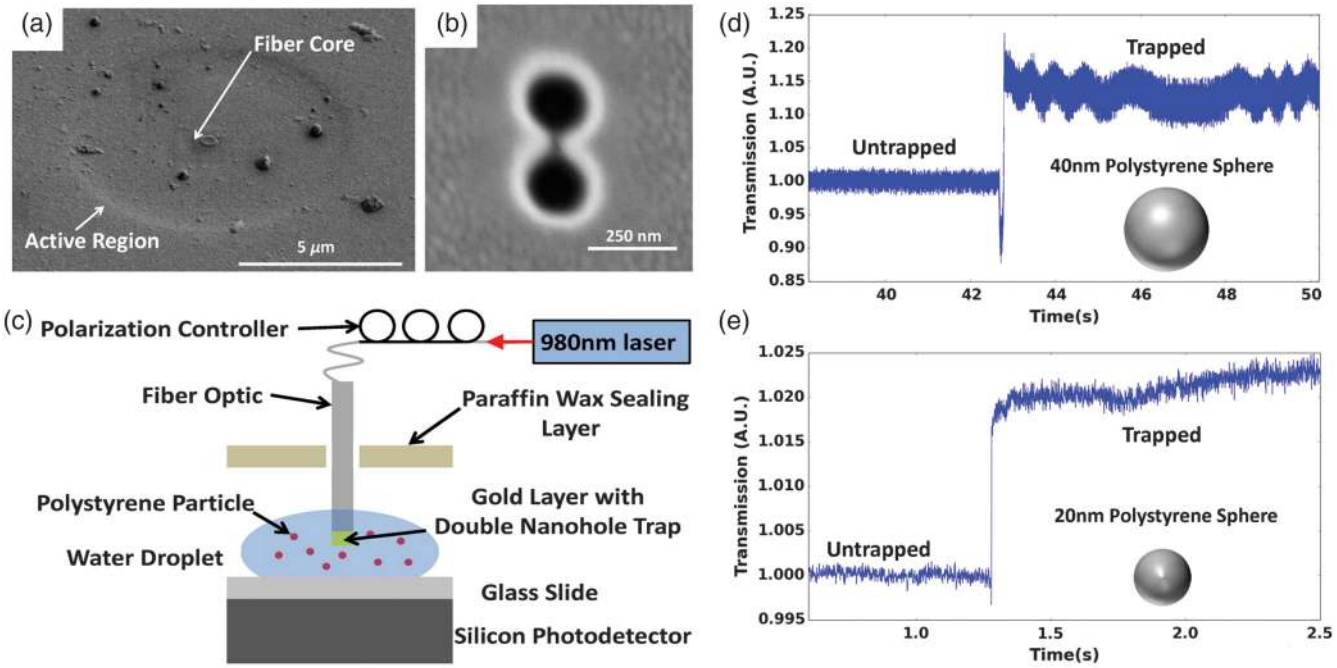

Fig. 13 Optical tweezers based on a double nanohole on the fiber endface.[272] (a) SEM image of the active region of the fiber. (b) SEM image of the finished double nanohole milled in the active region of the fiber. (c) Schematic illustration of the characterization setup of the optical tweezers. (d), (e) Trapping events for individual 40- and 20-nm diameter PS spheres, respectively, which are detected via the change in transmission. Copyright 2014, Optical Society of America.

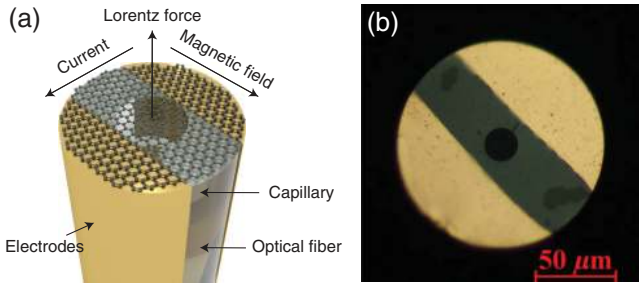

Fig. 14 NEMS on fiber tips. (a) Schematic of the optical fiber magnetometer based on a graphene NEMS. (b) Microscope image of the endface of the fiber sensor.

3.2.1 NEMS on fiber

Optical NEMSs are optical systems with adjustable or controllable mechanical components and are widespread in the fields of sensing and communications. Since the discovery of graphene, with its unique electronic and mechanical properties, several investigations have explored the integration of graphene NEMS on optical fiber tips. As shown in Fig. 14, Zheng et al.[67] demonstrated a miniature optical fiber current sensor based on a quasistatic graphene NEMS. The optical fiber was etched by an HF-water solution, forming a hole in the center of the fiber tip due to the faster etching speeds at the core area. Subsequently, a pair of Au electrodes was fabricated on opposite sides of the hole, which was covered by a free-standing graphene membrane. Due to the negative thermal expansion effect of graphene, the shape of the graphene membrane changed with the current-induced variation of temperature, which was detected using the reflection spectra of the sensor. An equivalent device configuration has been demonstrated for magnetic field sensing based on the Lorentz force.[275] Similarly, Liu et al.[49] fabricated an all-in-fiber current-driven Lorentz force magnetometer based on an NEMS consisting of a fiber-capillary-graphene-gold hybrid structure. The difference is that the graphene membrane was used principally to support a 100-nm-thick Au layer, which has a higher light reflection ratio, lower resistance, and better repeatability. The shape of the suspended graphene-gold-composite membrane changed with the applied Lorentz force, which was related to the propagating current in the magnetic field. By monitoring the reflection spectra of the sensor, the change in the magnetic field was detected with a sensitivity of 0.64 pm/mT and a response time of ~0.1 s.

3.2.2 Photoelectrical conversion

The integration of optoelectronic materials onto optical fibers is an effective way to overcome the limitations inherent to optical fiber materials. Recently, various kinds of photoelectric materials, such as quantum dots, nanotubes, perovskites, 2D materials, organic optoelectronic materials, and multiple-material heterostructures, have been exploited for on chip phototransistors, photodetectors, sensors, and solar cells among others.[276–280]

Photodetection. Similar to on-chip configurations, fiber-based photodetectors have been demonstrated successfully. As mentioned in Sec. 2.1.2, Chen et al.[38] developed a simple approach for fabricating electrodes on fibers with relatively high precision using lapping films and a tapered tungsten needle to construct two electrodes on opposite fiber sidewalls and facets. Then, a film of few-layer molybdenum disulfide (MoS_2) was bonded directly to the fiber electrode [Fig. 15(a)], demonstrating an all-in-FPD with a photoresponsivity of ~0.6 A W^{-1} at an incident light power of ~4.4 nW. Owing to the spatial asymmetry of the electrodes, the FPD worked at zero bias. To improve photodetection performance, FPDs with integrated perovskites-graphene hybrid structures have been proposed, as shown in Fig. 15(b). Aided by the high carrier mobility inside graphene and the high photosensitivity of perovskites, the FPD showed a photoresponsivity as high as 2×10^4 A W^{-1}.[164]

However, these FPDs can only detect visible light because of the limitations of the materials, hindering their application at communication frequencies. To resolve this issue, Xiong et al.[36] deployed a simple layer-by-layer transfer method to create a microscale multilayer graphene-MoS_2-WS_2 heterostructure film on fiber tip electrodes [Fig. 15(c)]. Due to the strong light absorption and the built-in electric field of the heterostructure, the FPD exhibits an ultrahigh photoresponsivity of $\sim 6.6 \times 10^7$ A W^{-1} and a relatively fast response time of ~7 ms at a wavelength of 400 nm. Moreover, the type-II staggered band alignments in the MoS_2-WS_2 heterostructure enables the FPD to sense infrared light, displaying a photoresponsivity of ~17.1 A W^{-1} at 1550 nm. Recently, a 2D covalent organic framework (COF)-graphene film was successfully integrated onto fiber electrodes using a similar approach, with the final structure utilized for gas sensing applications [Fig. 15(d)].[37]

We envision an all-in-fiber phototransistor with a three-electrode configuration on the fiber tip, consisting of a pair of drain-source electrodes and a transparent back gate electrode, which can adjust the semiconductor properties by controlling the gate voltage. This configuration should satisfy applications in both photoelectrical conversion and electro-optical modulation.

Photoelectrochemical analysis. The photoelectrochemical (PEC) process refers to the photoelectrical conversion of photoactive materials under illumination that forms electron–hole pairs at their interface, which will cause the oxidation–reduction reaction of the molecules or ions.[281] Owing to their light-guiding properties, optical fibers are an ideal platform for monitoring PEC reactions. For example, Esquivel et al. developed a TiO_2-based photoanode on the surface of a semiconductive modified optical fiber, thus allowing the construction of a PEC reactor via an internally illuminated approach. Using this configuration, the electro-Fenton photoelectrocatalytic oxidation process was studied to achieve total color removal of the azo dye Orange II (15 mg L^{-1}) and a 57% removal of total organic carbon within 60 min of the degradation time.[282] In addition, electro-optical nanoprobes based on tapered optical fibers may have application prospects in single-cell analysis.[283]

3.2.3 Optical modulation

The light propagating through a certain material can be modulated by external environmental factors, such as electric fields, optical fields, magnetic fields, temperature, and mechanical strain.[284,285] The small core and the engineerable endface or sidewall of optical fibers can offer tight optical confinement for enhancing light–material interactions, thus making optical fibers an ideal platform on which to develop modulators and lasers.[17,286,287]

Thermo-optic. With improvements to the processes used to attach electrodes on optical fiber tips, it is possible to develop

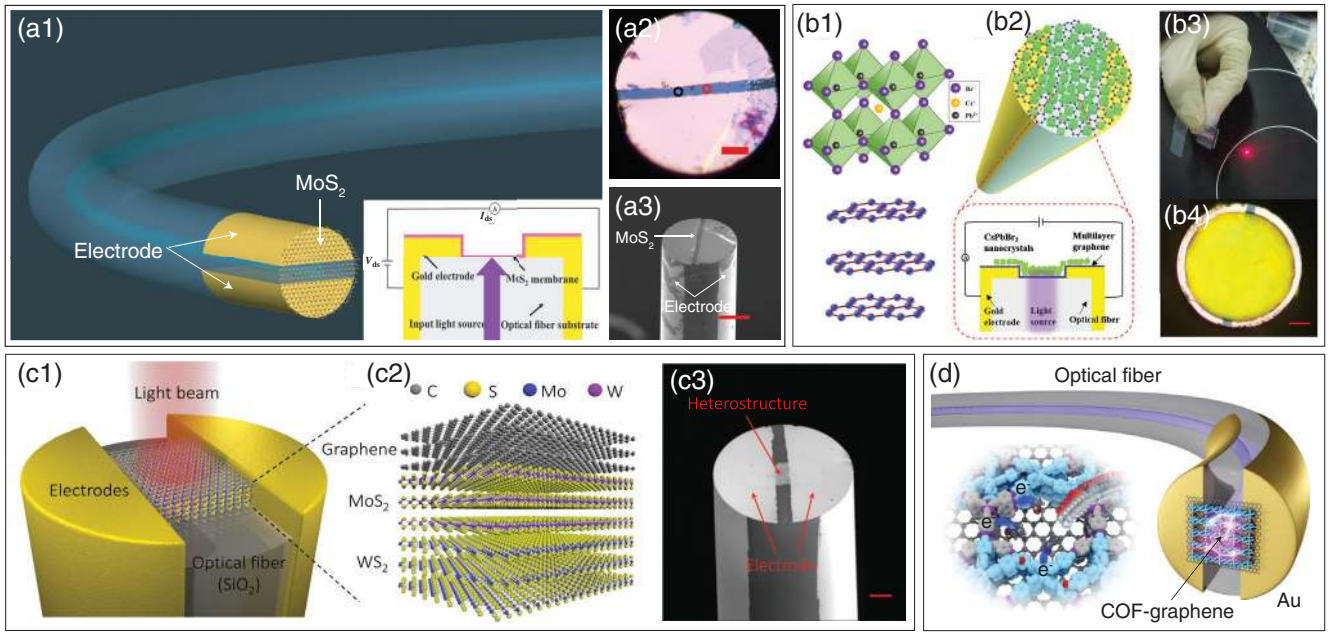

Fig. 15 All-in-FPD. (a) FPD integrated with a film of MoS_2.[38] (a1) Schematic of the FPD with a MoS_2 film deposited above the electrodes. Inset: The cross-sectional part of the FPD and the measurement setup. (a2) The optical microscope image of the FPD. The scale bar is 20 μm. (a3) The SEM image of the FPD. The scale bar is 50 μm. Reproduced with permission from the Royal Society of Chemistry. (b) High-sensitivity FPD with an integrated $CsPbBr_3$-graphene hybrid structure.[164] (b1), (b2) Schematic of the materials structures and device configuration of the FPD. (b3), (b4) Photograph and microscope image of an FPD. The scale bar is 20 μm. Copyright 2017, Optical Society of America. (c) Broadband FPD based on a graphene-MoS_2-WS_2 heterostructure.[36] (c1), (c2) Schematic representation of the FPD. (c3) SEM image of the FPD. The scale bar is 20 μm. Copyright 2018, WILEY-VCH Verlag GmbH & Co. KGaA, Weinheim. (d) Schematic view of the COF-graphene-based FPD, which can be used as a gas sensor. Inset: The gas molecule absorption and charge transfer at the surface of the COF-graphene film.[37] Copyright 2020, WILEY-VCH Verlag GmbH & Co. KGaA, Weinheim.

electro-optic and thermo-optic modulators on the fiber tips. For example, Li et al. demonstrated the active modulation of the nonlinear optical properties of a graphene-fiber-integrated device by varying the temperature of a graphene sheet electrically. The device was fabricated by bonding multilayer graphene directly onto a pair of fiber tip electrodes, with the result that they acted as a nanoheater as well as an adjustable saturable absorber. By tuning the applied electrical current from 0 to 9 mA, the temperature of the graphene was altered from ~300 to ~900 K, thus modifying the nonlinear optical absorption of the graphene from 2.3% to 0.9%. This graphene-based optical modulator was incorporated into a fiber laser circuit to demonstrate the controllable fiber laser's operation state (mode-locked or continuous-wave) and pulse.

Magneto-optic. The electron spin of nitrogen-vacancy (NV) color centers in diamonds enables the highly sensitive detection of weak magnetic fields, which can be manipulated by a frequency-modulated microwave field and initialized via laser radiation from the fiber core. Following this principle, Fedotov et al. reported optical fiber magnetic field imaging probes by attaching diamond microcrystals with NV centers to the fiber tip and integrating microwave transmission lines along the fibers. The 2D magnetic field was imaged by the probe, using the photoluminescence spin-readout return from the NV centers.[288–291]

In addition to advancements concerning the complexity of fiber tip electrode structures, high performance all-in-fiber devices, such as modulators, phototransistors, and Hall magnetic field sensors, will be developed in the future.

4 Conclusions and Outlook

LOF devices have made great progress so far in almost all aspects, ranging from theoretical calculation and device configuration design to fabrication techniques and measuring methods, with the ultimate aim of realizing integrated and miniaturized all-fiber systems. Growing technological demands bring great opportunities to explore new approaches for fiber functionalization and help the as-yet-unresolved challenges to be surmounted. The main challenge is to develop mass production processes and equipment for the integration of materials and structures on the platform of optical fiber endfaces, with reduced costs and increased yields. Meanwhile, the integration of certain complex traditional photonic and optoelectronic systems is another significant obstacle.

As regards future prospects, several trends and directions that show particular promise in this field include:

– First, multifunctional integration of traditional optoelectronic devices, both active and passive, onto fiber tips, thereby achieving a complete all-fiber module for light generation or signal processing.

– Second, the integration of complex electrode structures and auxiliary circuits on optical fiber endfaces, which can be applied as high-speed optical modulators, phototransistors, and sensors.

– Third, the integration of free space optical systems on fiber endfaces, thus realizing multiple functional all-fiber systems such as ultrathin imaging systems or spectrum conversion systems.

– Fourth, the integration of micro- and nanostructures on the endface of specific optical fibers (e.g., PCFs), realizing diversified functions that an ordinary optical fiber does not possess.

– Finally, the preparation of functional modules with reduced sizes onto the subwavelength-scale optical fiber tips for cell-level detection and *in vivo* biochemical monitoring.

Acknowledgments

This work was sponsored by the National Natural Science Foundation of China (61925502 and 61535005) and the National Key R&D Program of China (2017YFA0303700 and 2017YFA0700503). We thank Professor J. H. Chen for help in the preparation of the manuscript. The authors declare no competing interests.

References

1. A. F. Abouraddy et al., "Towards multimaterial multifunctional fibres that see, hear, sense and communicate," *Nat. Mater.* **6**, 336–347 (2007).
2. M. Bayindir et al., "Integrated fibres for self-monitored optical transport," *Nat. Mater.* **4**, 820–825 (2005).
3. O. Shapira et al., "Surface-emitting fiber lasers," *Opt. Express* **14**(9), 3929–3935 (2006).
4. A. Bedeloglu et al., "A photovoltaic fiber design for smart textiles," *Text. Res. J.* **80**(11), 1065–1074 (2009).
5. N. Podoliak et al., "Design of dual-core optical fibers with NEMS functionality," *Opt. Express* **22**(1), 1065–1076 (2014).
6. A. Canales et al., "Multifunctional fibers for simultaneous optical, electrical and chemical interrogation of neural circuits *in vivo*," *Nat. Biotechnol.* **33**, 277–284 (2015).
7. S. Egusa et al., "Multimaterial piezoelectric fibres," *Nat. Mater.* **9**, 643–648 (2010).
8. M. Fokine et al., "Integrated fiber Mach–Zehnder interferometer for electro-optic switching," *Opt. Lett.* **27**(18), 1643–1645 (2002).
9. W. Yan et al., "Microstructure tailoring of selenium-core multimaterial optoelectronic fibers," *Opt. Mater. Express* **7**(4), 1388–1397 (2017).
10. W. Yan et al., "Semiconducting nanowire-based optoelectronic fibers," *Adv. Mater.* **29**(27), 1700681 (2017).
11. W. Yan et al., "Advanced multimaterial electronic and optoelectronic fibers and textiles," *Adv. Mater.* **31**(1), 1802348 (2019).
12. W. Yan et al., "Thermally drawn advanced functional fibers: new Frontier of flexible electronics," *Mater. Today* **35**, 168–194 (2020).
13. L. Tong et al., "Subwavelength-diameter silica wires for low-loss optical wave guiding," *Nature* **426**, 816–819 (2003).
14. J.-H. Chen, D.-R. Li, and F. Xu, "Optical microfiber sensors: sensing mechanisms, and recent advances," *J. Lightwave Technol.* **37**(11), 2577–2589 (2019).
15. D. Pawar and S. N. Kale, "A review on nanomaterial-modified optical fiber sensors for gases, vapors and ions," *Mikrochim. Acta* **186**, 253 (2019).
16. H. Chen et al., "Review and perspective: sapphire optical fiber cladding development for harsh environment sensing," *Appl. Phys. Rev.* **5**(1), 011102 (2018).
17. E. J. Lee et al., "Active control of all-fibre graphene devices with electrical gating," *Nat. Commun.* **6**, 6851 (2015).
18. J. D. Zapata et al., "Efficient graphene saturable absorbers on D-shaped optical fiber for ultrashort pulse generation," *Sci. Rep.* **6**, 20644 (2016).
19. J. L. Kou et al., "Microfiber-based Bragg gratings for sensing applications: a review," *Sensors* **12**(7), 8861–8876 (2012).
20. S. Pissadakis, "Lab-in-a-fiber sensors: a review," *Microelectron. Eng.* **217**, 111105 (2019).
21. M. Pisco and A. Cusano, "Lab-on-fiber technology: a roadmap toward multifunctional plug and play platforms," *Sensors* **20**(17), 4705 (2020).
22. Q. Wang and L. Wang, "Lab-on-fiber: plasmonic nano-arrays for sensing," *Nanoscale* **12**(14), 7485–7499 (2020).
23. P. Vaiano et al., "Lab on fiber technology for biological sensing applications," *Laser Photonics Rev.* **10**(6), 922–961 (2016).
24. A. Ricciardi et al., "Lab-on-fiber technology: a new vision for chemical and biological sensing," *Analyst* **140**(24), 8068–8079 (2015).
25. G. Kostovski, P. R. Stoddart, and A. Mitchell, "The optical fiber tip: an inherently light-coupled microscopic platform for micro- and nanotechnologies," *Adv. Mater.* **26**(23), 3798–3820 (2014).
26. M. Consales, M. Pisco, and A. Cusano, "Lab-on-fiber technology: a new avenue for optical nanosensors," *Photonic Sensors* **2**, 289–314 (2012).
27. R. He et al., "Integration of gigahertz-bandwidth semiconductor devices inside microstructured optical fibres," *Nat. Photonics* **6**, 174–179 (2012).
28. A. F. Abouraddy et al., "Large-scale optical-field measurements with geometric fibre constructs," *Nat. Mater.* **5**, 532–536 (2006).
29. R. Raabe et al., "No enhancement of fusion probability by the neutron halo of ^{6}He," *Nature* **431**, 823–826 (2004).
30. B. Temelkuran et al., "Wavelength-scalable hollow optical fibres with large photonic bandgaps for CO_2 laser transmission," *Nature* **420**, 650–653 (2002).
31. S. A. Maier, *Plasmonics: Fundamentals and Applications*, Springer (2007).
32. K. I. Mullen and K. T. Carron, "Surface-enhanced Raman spectroscopy with abrasively modified fiber optic probes," *Anal. Chem.* **63**(19), 2196–2199 (1991).
33. W. H. C. Viets, "Comparison of fibre-optic SERS sensors with differently prepared tips," *Sens. Actuators B* **51**(1–3), 92–99 (1998).
34. T. Grosjean et al., "Fiber microaxicons fabricated by a polishing technique for the generation of Bessel-like beams," *Appl. Opt.* **46**(33), 8061–8067 (2007).
35. C. Li et al., "Manipulation of nonlinear optical properties of graphene bonded fiber devices by thermally engineering Fermi-Dirac distribution," *Adv. Opt. Mater.* **5**(21), 1700630 (2017).
36. Y.-F. Xiong et al., "Broadband optical-fiber-compatible photodetector based on a graphene-MoS_2-WS_2 heterostructure with a synergetic photogenerating mechanism," *Adv. Electron. Mater.* **5**(1), 1800562 (2019).
37. Y. Xiong et al., "Ultrahigh responsivity photodetectors of 2D covalent organic frameworks integrated on graphene," *Adv. Mater.* **32**(9), 1907242 (2020).
38. J. H. Chen et al., "Towards an all-in fiber photodetector by directly bonding few-layer molybdenum disulfide to a fiber facet," *Nanoscale* **9**(10), 3424–3428 (2017).
39. F. A. Bruno et al., "Opto-mechanical lab-on-fiber accelerometers," *J. Lightwave Technol.* **38**(7), 1998–2009 (2020).
40. S. V. Beekmans et al., "Minimally invasive micro-indentation: mapping tissue mechanics at the tip of an 18G needle," *Sci. Rep.* **7**, 11364 (2017).

41. H. van Hoorn et al., "Local dynamic mechanical analysis for heterogeneous soft matter using ferrule-top indentation," *Soft Matter* **12**(12), 3066–3073 (2016).
42. M. Pisco et al., "Opto-mechanical lab-on-fibre seismic sensors detected the Norcia earthquake," *Sci. Rep.* **8**, 6680 (2018).
43. J.-Y. Rauch et al., "Smallest microhouse in the world, assembled on the facet of an optical fiber by origami and welded in the μRobotex nanofactory," *J. Vac. Sci. Technol. A* **36**, 041601 (2018).
44. F. Guo et al., "High-sensitivity, high-frequency extrinsic Fabry–Perot interferometric fiber-tip sensor based on a thin silver diaphragm," *Opt. Lett.* **37**(9), 1505–1507 (2012).
45. J. Ma et al., "High-sensitivity fiber-tip pressure sensor with graphene diaphragm," *Opt. Lett.* **37**(13), 2493–2495 (2012).
46. Y. Wang et al., "Compressible fiber optic micro-Fabry–Perot cavity with ultra-high pressure sensitivity," *Opt. Express* **21**(12), 14084–14089 (2013).
47. J. Xu et al., "Suppression of parasitic interference in a fiber-tip Fabry–Perot interferometer for high-pressure measurements," *Opt. Express* **26**(22), 28178–28186 (2018).
48. Z. Yizheng and W. Anbo, "Miniature fiber-optic pressure sensor," *IEEE Photonics Technol. Lett.* **17**(2), 447–449 (2005).
49. Z.-Y. Liu, H.-Q. Cao, and F. Xu, "Fiber-optic Lorentz force magnetometer based on a gold-graphene composite membrane," *Appl. Phys. Lett.* **112**(20), 203504 (2018).
50. Y. Zhao et al., "Optical fiber axial contact force sensor based on bubble-expanded Fabry–Pérot interferometer," *Sens. Actuators A* **272**, 318–324 (2018).
51. K.-C. Fan et al., "Experimental study of fabricating a microball tip on an optical fibre," *J. Opt. A Pure Appl. Opt.* **8**(9), 782–787 (2006).
52. L. Collot et al., "Very high-Q whispering-gallery mode resonances observed on fused silica microspheres," *Europhys. Lett.* **23**(5), 327–334 (1993).
53. M. L. Gorodetsky, A. A. Savchenkov, and V. S. Ilchenko, "Ultimate Q of optical microsphere resonators," *Opt. Lett.* **21**(7), 453–455 (1996).
54. M. Kimura and K. Toshima, "Vibration sensor using optical-fiber cantilever with bulb-lens," *Sens. Actuators A* **66**(1–3), 178–183 (1998).
55. J. Laine, B. E. Little, and H. A. Haus, "Etch-eroded fiber coupler for whispering-gallery-mode excitation in high-Q silica microspheres," *IEEE Photonics Technol. Lett.* **11**(11), 1429–1430 (1999).
56. S.-K. Eah, W. Jhe, and Y. Arakawa, "Nearly diffraction-limited focusing of a fiber axicon microlens," *Rev. Sci. Instrum.* **74**(11), 4969–4971 (2003).
57. H. J. Kbashi, "Fabrication of submicron-diameter and taper fibers using chemical etching," *J. Mater. Sci. Technol.* **28**(4), 308–312 (2012).
58. T. Saiki et al., "Tailoring a high-transmission fiber probe for photon scanning tunneling microscope," *Appl. Phys. Lett.* **68**, 2612–2614 (1996).
59. G. Eisenstein and D. Vitello, "Chemically etched conical microlenses for coupling single-mode lasers into single-mode fibers," *Appl. Opt.* **21**(19), 3470–3474 (1982).
60. T. Yatsui, M. Kourogi, and M. Ohtsu, "Increasing throughput of a near-field optical fiber probe over 1000 times by the use of a triple-tapered structure," *Appl. Phys. Lett.* **73**(15), 2090–2092 (1998).
61. T. Saiki and K. Matsuda, "Near-field optical fiber probe optimized for illumination–collection hybrid mode operation," *Appl. Phys. Lett.* **74**(19), 2773–2775 (1999).
62. P. Hoffmann, B. Dutoit, and R.-P. Salathe, "Comparison of mechanically drawn and protection layer chemically etchedoptical fiber tips," *Ultramicroscopy* **61**(1–4), 165–170 (1995).
63. S. K. Mondal et al., "Optical fiber nanoprobe preparation for near-field optical microscopy by chemical etching under surface tension and capillary action," *Opt. Express* **17**(22), 19470–19475 (2009).
64. K. Maruyama et al., "Fabrication and characterization of a nanometer-sized optical fiber electrode based on selective chemical etching for scanning electrochemical/optical microscopy," *Anal. Chem.* **78**(6), 1904–1912 (2006).
65. Z. Wang et al., "Optically addressable array of optomechanically compliant glass nanospikes on the endface of a soft-glass photonic crystal fiber," *ACS Photonics* **6**(11), 2942–2948 (2019).
66. D. J. White and P. R. Stoddart, "Nanostructured optical fiber with surface-enhanced Raman scattering functionality," *Opt. Lett.* **30**(6), 598–600 (2005).
67. B.-C. Zheng et al., "Miniature optical fiber current sensor based on a graphene membrane," *Laser Photonics Rev.* **9**(5), 517–522 (2015).
68. S. Cabrini et al., "Axicon lens on optical fiber forming optical tweezers, made by focused ion beam milling," *Microelectron. Eng.* **83**(4–9), 804–807 (2006).
69. F. Schiappelli, "Efficient fiber-to-waveguide coupling by a lens on the end of the optical fiber fabricated by focused ion beam milling," *Microelectron. Eng.* **73-74**, 397–404 (2004).
70. D. Iannuzzi et al., "Fiber-top atomic force microscope," *Rev. Sci. Instrum.* **77**(10), 106105 (2006).
71. D. Iannuzzi et al., "Monolithic fiber-top sensor for critical environments and standard applications," *Appl. Phys. Lett.* **88**(5), 053501 (2006).
72. C. Liberale et al., "Miniaturized all-fibre probe for three-dimensional optical trapping and manipulation," *Nat. Photonics* **1**, 723–727 (2007).
73. G. F. S. Andrade et al., "Surface-enhanced resonance Raman scattering (SERRS) using Au nanohole arrays on optical fiber tips," *Plasmonics* **8**, 1113–1121 (2013).
74. S. Kang et al., "Subwavelength plasmonic lens patterned on a composite optical fiber facet for quasi-one-dimensional Bessel beam generation," *Appl. Phys. Lett.* **98**(24), 241103 (2011).
75. Y. Zhao, "All-fiber vibration sensor based on nano-wire grid polarizer," *Opt. Eng.* **51**(5), 050504 (2012).
76. A. Dhawan and J. F. Muth, "Engineering surface plasmon based fiber-optic sensors," *Mater. Sci. Eng. B* **149**(3), 237–241 (2008).
77. A. Dhawan, M. D. Gerhold, and J. F. Muth, "Plasmonic structures based on subwavelength apertures for chemical and biological sensing applications," *IEEE Sens. J.* **8**(6), 942–950 (2008).
78. M. Principe et al., "Optical fiber meta-tips," *Light Sci. Appl.* **6**, e16226 (2017).
79. V. Savinov and N. I. Zheludev, "High-quality metamaterial dispersive grating on the facet of an optical fiber," *Appl. Phys. Lett.* **111**(9), 091106 (2017).
80. A. Micco et al., "Optical fiber tip templating using direct focused ion beam milling," *Sci. Rep.* **5**, 15935 (2015).
81. W. Shin et al., "Microstructured fiber end surface grating for coarse WDM signal monitoring," *IEEE Photonics Technol. Lett.* **19**(8), 550–552 (2007).
82. J. K. Kim et al., "Fabrication of micro Fresnel zone plate lens on a mode-expanded hybrid optical fiber using a femtosecond laser ablation system," *IEEE Photonics Technol. Lett.* **21**(1), 21–23 (2009).
83. X. Lan et al., "Surface-enhanced Raman-scattering fiber probe fabricated by femtosecond laser," *Opt. Lett.* **34**(15), 2285–2287 (2009).
84. X. Ma et al., "Surface-enhanced Raman scattering sensor on an optical fiber probe fabricated with a femtosecond laser," *Sensors* **10**(12), 11064–11071 (2010).
85. Y. Lin, J. Guo, and R. G. Lindquist, "Demonstration of an ultra-wideband optical fiber inline polarizer with metal nano-grid on the fiber tip," *Opt. Express* **17**(20), 17849–17854 (2009).
86. Y. Lin et al., "E-beam patterned gold nanodot arrays on optical fiber tips for localized surface plasmon resonance biochemical sensing," *Sensors* **10**(10), 9397–9406 (2010).

87. M. Sanders et al., "An enhanced LSPR fiber-optic nanoprobe for ultrasensitive detection of protein biomarkers," *Biosens. Bioelectron.* **61**, 95–101 (2014).
88. M. Consales et al., "Lab-on-fiber technology: toward multifunctional optical nanoprobes," *ACS Nano* **6**(4), 3163–3170 (2012).
89. S. Feng et al., "A miniaturized sensor consisting of concentric metallic nanorings on the end facet of an optical fiber," *Small* **8**(12), 1937–1944 (2012).
90. M. Sasaki et al., "Direct photolithography on optical fiber end," *Jpn. J. Appl. Phys.* **41**(Part 1), 4350–4355(2002).
91. E. G. Johnson et al., "Fabrication of micro optics on coreless fiber segments," *Appl. Opt.* **42**(5), 785–791 (2003).
92. A. Petrušis et al., "The align-and-shine technique for series production of photolithography patterns on optical fibres," *J. Micromech. Microeng.* **19**(4), 047001 (2009).
93. J. B. Kim and K. H. Jeong, "Batch fabrication of functional optical elements on a fiber facet using DMD based maskless lithography," *Opt. Express* **25**(14), 16854–16859 (2017).
94. S. Choi et al., "Interferometric inscription of surface relief gratings on optical fiber using azo polymer film," *Appl. Phys. Lett.* **83**(6), 1080–1082 (2003).
95. S. Feng et al., "Fiber coupled waveguide grating structures," *Appl. Phys. Lett.* **96**(13), 133101 (2010).
96. X. Yang et al., "Nanopillar array on a fiber facet for highly sensitive surface-enhanced Raman scattering," *Opt. Express* **20**(22), 24819–24826 (2012).
97. J. Chandrappan et al., "Optical coupling methods for cost-effective polymer optical fiber communication," *IEEE Trans. Compon. Packag. Technol.* **32**(3), 593–599 (2009).
98. C. Florea et al., "Reduced Fresnel losses in chalcogenide fibers obtained through fiber-end microstructuring," *Appl. Opt.* **50**(1), 17–21 (2011).
99. J. Sanghera et al., "Reduced Fresnel losses in chalcogenide fibers by using anti-reflective surface structures on fiber end faces," *Opt. Express* **18**(25), 26760–26768 (2010).
100. A. V. Volkov et al., "Studying fabrication errors of the diffraction grating on the end face of a silver-halide fiber," *Opt. Memory Neural Networks* **16**, 263–268 (2007).
101. H. Sakata and A. Imada, "Lensed plastic optical fiber employing concave end filled with high-index resin," *J. Lightwave Technol.* **20**(4), 638–642 (2002).
102. G. Kostovski et al., "Nanoimprinted optical fibres: biotemplated nanostructures for SERS sensing," *Biosens. Bioelectron.* **24**(5), 1531–1535 (2009).
103. J. Viheriälä et al., "Fabrication of surface reliefs on facets of singlemode optical fibres using nanoimprint lithography," *Electron. Lett.* **43**(3), 150–151 (2007).
104. S. Scheerlinck et al., "Metal grating patterning on fiber facets by UV-based nano imprint and transfer lithography using optical alignment," *J. Lightwave Technol.* **27**(10), 1415–1420 (2009).
105. Y. Kanamori, M. Okochi, and K. Hane, "Fabrication of antireflection subwavelength gratings at the tips of optical fibers using UV nanoimprint lithography," *Opt. Express* **21**(1), 322–328 (2013).
106. S. Scheerlinck et al., "Flexible metal grating based optical fiber probe for photonic integrated circuits," *Appl. Phys. Lett.* **92**(3), 031104 (2008).
107. G. Calafiore et al., "Nanoimprint of a 3D structure on an optical fiber for light wavefront manipulation," *Nanotechnology* **27**(37), 375301 (2016).
108. G. Calafiore et al., "Campanile near-field probes fabricated by nanoimprint lithography on the facet of an optical fiber," *Sci. Rep.* **7**(1), 1651 (2017).
109. G. Kostovski et al., "Sub-15 nm optical fiber nanoimprint lithography: a parallel, self-aligned and portable approach," *Adv. Mater.* **23**(4), 531–535 (2011).
110. M. Prasciolu et al., "Design and fabrication of on-fiber diffractive elements for fiber-waveguide coupling by means of e-beam lithography," *Microelectron. Eng.* **67-68**, 169–174 (2003).
111. A. Ricciardi et al., "Lab-on-fiber devices as an all around platform for sensing," *Opt. Fiber Technol.* **19**(6), 772–784 (2013).
112. A. Ricciardi et al., "Versatile optical fiber nanoprobes: from plasmonic biosensors to polarization-sensitive devices," *ACS Photonics* **1**(1), 69–78 (2013).
113. Y. Lin, Y. Zou, and R. G. Lindquist, "A reflection-based localized surface plasmon resonance fiber-optic probe for biochemical sensing," *Biomed. Opt. Express* **2**(3), 478–484 (2011).
114. Z. Huang et al., "Tapered optical fiber probe assembled with plasmonic nanostructures for surface-enhanced Raman scattering application," *ACS Appl. Mater. Interfaces* **7**(31), 17247–17254 (2015).
115. P. D. Palma et al., "Self-assembled colloidal photonic crystal on the fiber optic tip as a sensing probe," *IEEE Photonics J.* **9**(2), 7102511 (2017).
116. F. Galeotti, M. Pisco, and A. Cusano, "Self-assembly on optical fibers: a powerful nanofabrication tool for next generation 'lab-on-fiber' optrodes," *Nanoscale* **10**(48), 22673–22700 (2018).
117. H. H. Jeong et al., "Real-time label-free immunoassay of interferon-gamma and prostate-specific antigen using a fiber-optic localized surface plasmon resonance sensor," *Biosens. Bioelectron.* **39**(1), 346–351 (2013).
118. B. Sciacca and T. M. Monro, "Dip biosensor based on localized surface plasmon resonance at the tip of an optical fiber," *Langmuir* **30**(3), 946–954 (2014).
119. Y. Liu et al., "Highly sensitive fibre surface-enhanced Raman scattering probes fabricated using laser-induced self-assembly in a meniscus," *Nanoscale* **8**(20), 10607–10614 (2016).
120. F. L. Yap et al., "Nanoparticle cluster arrays for high-performance SERS through directed self-assembly on flat substrates and on optical fibers," *ACS Nano* **6**(3), 2056–2070 (2012).
121. M. Pisco et al., "Miniaturized sensing probes based on metallic dielectric crystals self-assembled on optical fiber tips," *ACS Photonics* **1**(10), 917–927 (2014).
122. M. Pisco et al., "Nanosphere lithography for optical fiber tip nanoprobes," *Light Sci. Appl.* **6**(5), e16229 (2017).
123. I. Antohe et al., "Nanoscale patterning of gold-coated optical fibers for improved plasmonic sensing," *Nanotechnology* **28**(21), 215301 (2017).
124. G. Quero et al., "Nanosphere lithography on fiber: towards engineered lab-on-fiber SERS optrodes," *Sensors* **18**(3), 680 (2018).
125. J. R. Rabeau et al., "Diamond chemical-vapor deposition on optical fibers for fluorescence waveguiding," *Appl. Phys. Lett.* **86**(13), 134104 (2005).
126. H. Chen et al., "Transition-metal dichalcogenides heterostructure saturable absorbers for ultrafast photonics," *Opt. Lett.* **42**(21), 4279–4282 (2017).
127. C. Huang et al., "Fabrication of high-temperature temperature sensor based on dielectric multilayer film on sapphire fiber tip," *Sens. Actuators A* **232**, 99–102 (2015).
128. D. W. Lee et al., "Sapphire fiber high-temperature tip sensor with multilayer coating," *IEEE Photonics Technol. Lett.* **27**(7), 741–743 (2015).
129. D. Tan et al., "Reduction in feature size of two-photon polymerization using SCR500," *Appl. Phys. Lett.* **90**(7), 071106 (2007).
130. M. Malinauskas et al., "Ultrafast laser processing of materials: from science to industry," *Light Sci. Appl.* **5**(8), e16133 (2016).
131. H. E. Williams et al., "Fabrication of three-dimensional micro-photonic structures on the tip of optical fibers using SU-8," *Opt. Express* **19**(23), 22910–22922 (2011).
132. T. Gissibl et al., "Sub-micrometre accurate free-form optics by three-dimensional printing on single-mode fibres," *Nat. Commun.* **7**, 11763 (2016).
133. V. Hahn et al., "Polarizing beam splitter integrated onto an optical fiber facet," *Opt. Express* **26**(25), 33148–33157 (2018).
134. C. Liberale et al., "Micro-optics fabrication on top of optical fibers using two-photon lithography," *IEEE Photonics Technol. Lett.* **22**(7), 474–476 (2010).

135. M. Malinauskas et al., "Femtosecond laser polymerization of hybrid/integrated micro-optical elements and their characterization," *J. Opt.* **12**(12), 124010 (2010).
136. M. Malinauskas et al., "3D microoptical elements formed in a photostructurable germanium silicate by direct laser writing," *Opt. Lasers Eng.* **50**(12), 1785–1788 (2012).
137. S. Bianchi et al., "Focusing and imaging with increased numerical apertures through multimode fibers with micro-fabricated optics," *Opt. Lett.* **38**(23), 4935–4938 (2013).
138. M. Kowalczyk, J. Haberko, and P. Wasylczyk, "Microstructured gradient-index antireflective coating fabricated on a fiber tip with direct laser writing," *Opt. Express* **22**(10), 12545–12550 (2014).
139. H. Huang et al., "Fabrication of micro-axicons using direct-laser writing," *Opt. Express* **22**(9), 11035–11042 (2014).
140. T. Gissibl, M. Schmid, and H. Giessen, "Spatial beam intensity shaping using phase masks on single-mode optical fibers fabricated by femtosecond direct laser writing," *Optica* **3**(4), 448–451 (2016).
141. H. Wei, M. Chen, and S. Krishnaswamy, "Three-dimensional-printed Fabry–Perot interferometer on an optical fiber tip for a gas pressure sensor," *Appl. Opt.* **59**(7), 2173–2178 (2020).
142. T. Gissibl et al., "Two-photon direct laser writing of ultracompact multi-lens objectives," *Nat. Photonics* **10**(8), 554–560 (2016).
143. Z. Xie et al., "Demonstration of a 3D radar-like SERS sensor micro- and nanofabricated on an optical fiber," *Adv. Opt. Mater.* **3**(9), 1232–1239 (2015).
144. H. Wang et al., "A miniaturized optical fiber microphone with concentric nanorings grating and microsprings structured diaphragm," *Opt. Laser Technol.* **78**(Part A), 110–115 (2016).
145. J. A. Kim et al., "Fiber-optic SERS probes fabricated using two-photon polymerization for rapid detection of bacteria," *Adv. Opt. Mater.* **8**(9), 1901934 (2020).
146. S. Zhang et al., "High-Q polymer microcavities integrated on a multicore fiber facet for vapor sensing," *Adv. Opt. Mater.* **7**(20), 1900602 (2019).
147. Q. Liu et al., "'Optical tentacle' of suspended polymer microrings on a multicore fiber facet for vapor sensing," *Opt. Express* **28**(8), 11730–11741 (2020).
148. M. Yao et al., "Optical 3D μ-printing of ferrule-top polymer suspended-mirror devices," in *IEEE SENSORS* (2016).
149. J. Wu et al., "*In situ* μ-printed optical fiber-tip CO_2 sensor using a photocrosslinkable poly(ionic liquid)," *Sens. Actuators B* **259**, 833–839 (2018).
150. M. Yao et al., "Optically 3-D μ-printed ferrule-top polymer suspended-mirror devices," *IEEE Sens. J.* **17**(22), 7257–7261 (2017).
151. M. Yao et al., "Optical fiber-tip sensors based on *in-situ* microprinted polymer suspended-microbeams," *Sensors* **18**(6), 1825 (2018).
152. O. Soppera, C. Turck, and D. J. Lougnot, "Fabrication of micro-optical devices by self-guiding photopolymerization in the near IR," *Opt. Lett.* **34**(4), 461–463 (2009).
153. O. Soppera, S. Jradi, and D. J. Lougnot, "Photopolymerization with microscale resolution: influence of the physico-chemical and photonic parameters," *J. Polymer Sci. Part A* **46**(11), 3783–3794 (2008).
154. R. Bachelot et al., "Integration of micrometer-sized polymer elements at the end of optical fibers by free-radical photopolymerization," *Appl. Opt.* **40**(32), 5860–5871 (2001).
155. M. Hocine et al., "End-of-fiber polymer tip: manufacturing and modeling," *Synth. Met.* **127**(1–3), 313–318 (2002).
156. L. Xiao et al., "Photopolymer microtips for efficient light coupling between single-mode fibers and photonic crystal fibers," *Opt. Lett.* **31**(12), 1791–1793 (2006).
157. C. Pang et al., "Enhanced light coupling in sub-wavelength single-mode silicon on insulator waveguides," *Opt. Express* **17**(9), 6939–6945 (2009).
158. S. Valkai, L. Oroszi, and P. Ormos, "Optical tweezers with tips grown at the end of fibers by photopolymerization," *Appl. Opt.* **48**(15), 2880–2883 (2009).
159. C. Shi et al., "A double substrate 'sandwich' structure for fiber surface enhanced Raman scattering detection," *Appl. Phys. Lett.* **92**(10), 103107 (2008).
160. Q. Bao et al., "Atomic-layer graphene as a saturable absorber for ultrafast pulsed lasers," *Adv. Funct. Mater.* **19**(19), 3077–3083 (2009).
161. K. Wu et al., "High-performance mode-locked and Q-switched fiber lasers based on novel 2D materials of topological insulators, transition metal dichalcogenides and black phosphorus: review and perspective (invited)," *Opt. Commun.* **406**, 214–229 (2018).
162. F. Wang et al., "Wideband-tuneable, nanotube mode-locked, fibre laser," *Nat. Nanotechnol.* **3**(12), 738–742 (2008).
163. S. Y. Set et al., "Ultrafast fiber pulsed lasers incorporating carbon nanotubes," *IEEE J. Sel. Top. Quantum Electron.* **10**(1), 137–146 (2004).
164. J.-H. Chen et al., "High-sensitivity optical-fiber-compatible photodetector with an integrated $CsPbBr_3$–graphene hybrid structure," *Optica* **4**(8), 835–838 (2017).
165. V. Calero et al., "An ultra wideband-high spatial resolution-compact electric field sensor based on lab-on-fiber technology," *Sci. Rep.* **9**, 8058 (2019).
166. E. J. Smythe et al., "Optical antenna arrays on a fiber facet for *in situ* surface-enhanced Raman scattering detection," *Nano Lett.* **9**(3), 1132–1138 (2009).
167. E. J. Smythe et al., "A technique to transfer metallic nanoscale patterns to small and non-planar surfaces," *ACS Nano* **3**(1), 59–65 (2009).
168. D. J. Lipomi et al., "Patterning the tips of optical fibers with metallic nanostructures using nanoskiving," *Nano Lett.* **11**(2), 632–636 (2011).
169. I. W. Jung et al., "Highly sensitive monolithic silicon photonic crystal fiber tip sensor for simultaneous measurement of refractive index and temperature," *J. Lightwave Technol.* **29**(9), 1367–1374 (2011).
170. B. Wang et al., "Photonic crystal cavity on optical fiber facet for refractive index sensing," *Opt. Lett.* **37**(5), 833–835 (2012).
171. X. He et al., "Plasmonic crystal cavity on single-mode optical fiber end facet for label-free biosensing," *Appl. Phys. Lett.* **108**(23), 231105 (2016).
172. G. Shambat et al., "Optical fiber tips functionalized with semiconductor photonic crystal cavities," *Appl. Phys. Lett.* **99**(19), 191102 (2011).
173. G. Shambat et al., "A photonic crystal cavity-optical fiber tip nanoparticle sensor for biomedical applications," *Appl. Phys. Lett.* **100**(21), 213702 (2012).
174. P. Jia and J. Yang, "A plasmonic optical fiber patterned by template transfer as a high-performance flexible nanoprobe for real-time biosensing," *Nanoscale* **6**(15), 8836–8843 (2014).
175. P. Jia and J. Yang, "Integration of large-area metallic nanohole arrays with multimode optical fibers for surface plasmon resonance sensing," *Appl. Phys. Lett.* **102**(24), 243107 (2013).
176. P. Jia et al., "Quasiperiodic nanohole arrays on optical fibers as plasmonic sensors: fabrication and sensitivity determination," *ACS Sens.* **1**(8), 1078–1083 (2016).
177. J. Yu et al., "Electrochemical plasmonic optical fiber probe for real-time insight into coreactant electrochemiluminescence," *Sens. Actuators B* **321**, 128469 (2020).
178. E. Zhao et al., "Localized surface plasmon resonance sensing structure based on gold nanohole array on beveled fiber edge," *Nanotechnology* **28**(43), 435504 (2017).
179. Y. Liu et al., "Simple and low-cost plasmonic fiber-optic probe as SERS and biosensing platform," *Adv. Opt. Mater.* **7**(19), 1900337 (2019).
180. C. L. Arce et al., "Silicon-on-insulator microring resonator sensor integrated on an optical fiber facet," *IEEE Photonics Technol. Lett.* **23**(13), 890–892 (2011).

181. C. Li et al., "Nondestructive and *in situ* determination of graphene layers using optical fiber Fabry–Perot interference," *Meas. Sci. Technol.* **28**(2), 025206 (2017).
182. C.-L. Zhang et al., "Lab-on-tip based on photothermal microbubble generation for concentration detection," *Sens. Actuators B* **255**(Part 3), 2504–2509 (2018).
183. M. Giaquinto et al., "Cavity-enhanced lab-on-fiber technology: toward advanced biosensors and nano-opto-mechanical active devices," *ACS Photonics* **6**(12), 3271–3280 (2019).
184. A. A. Said et al., "Carving fiber-top cantilevers with femtosecond laser micromachining," *J. Micromech. Microeng.* **18**(3), 035005 (2008).
185. B. Sun et al., "Simultaneous measurement of pressure and temperature by employing Fabry–Perot interferometer based on pendant polymer droplet," *Opt. Express* **23**(3), 1906–1911 (2015).
186. H. Won Baac et al., "Carbon nanotube composite optoacoustic transmitters for strong and high frequency ultrasound generation," *Appl. Phys. Lett.* **97**(23), 234104 (2010).
187. R. Ansari et al., "All-optical forward-viewing photoacoustic probe for high-resolution 3D endoscopy," *Light Sci. Appl.* **7**(1), 75 (2018).
188. C. Li, X. Peng, and J. Liu, "Fiber-tip photoacoustic probe with MoS_2-PDMS composite coating for temperature and density-induced ultrasonic speed tuning," *OSA Continuum* **1**(2), 488–495 (2018).
189. E. Zhang and P. Beard, "A miniature all-optical photoacoustic imaging probe," *Proc. SPIE* **7899**, 78991F (2011).
190. J. A. Guggenheim et al., "Ultrasensitive plano-concave optical microresonators for ultrasound sensing," *Nat. Photonics* **11**(11), 714–719 (2017).
191. R. J. Colchester et al., "Laser-generated ultrasound with optical fibres using functionalised carbon nanotube composite coatings," *Appl. Phys. Lett.* **104**(17), 173502 (2014).
192. S. Noimark et al., "Carbon-nanotube-PDMS composite coatings on optical fibers for all-optical ultrasound imaging," *Adv. Funct. Mater.* **26**(46), 8390–8396 (2016).
193. M. C. Finlay et al., "Through-needle all-optical ultrasound imaging *in vivo*: a preclinical swine study," *Light Sci. Appl.* **6**, e17103 (2017).
194. A. Koshelev et al., "High refractive index Fresnel lens on a fiber fabricated by nanoimprint lithography for immersion applications," *Opt. Lett.* **41**(15), 3423–3426 (2016).
195. J. Kim et al., "Achievement of large spot size and long collimation length using UV curable self-assembled polymer lens on a beam expanding core-less silica fiber," *IEEE Photonics Technol. Lett.* **16**(11), 2499–2501 (2004).
196. K. Kyung-Rok, C. Selee, and K. Oh, "Refractive microlens on fiber using UV-curable fluorinated acrylate polymer by surface-tension," *IEEE Photonics Technol. Lett.* **15**(8), 1100–1102 (2003).
197. A. Tuniz and M. A. Schmidt, "Interfacing optical fibers with plasmonic nanoconcentrators," *Nanophotonics* **7**(7), 1279–1298 (2018).
198. L. Kong et al., "Protruding-shaped SiO_2-microtip: from fabrication innovation to microphotonic device construction," *Opt. Lett.* **44**(14), 3514–3517 (2019).
199. T. Udem, R. Holzwarth, and T. W. Hänsch, "Optical frequency metrology," *Nature* **416**, 233–237 (2002).
200. C. Xu and F. W. Wise, "Recent advances in fiber lasers for nonlinear microscopy," *Nat. Photonics* **7**, 875–882 (2013).
201. P. Grelu and N. Akhmediev, "Dissipative solitons for mode-locked lasers," *Nat. Photonics* **6**, 84–92 (2012).
202. S. V. Smirnov, S. M. Kobtsev, and S. V. Kukarin, "Efficiency of non-linear frequency conversion of double-scale pico-femtosecond pulses of passively mode-locked fiber laser," *Opt. Express* **22**(1), 1058–1064 (2014).
203. P. Cheng et al., "Mode-locked and Q-switched mode-locked fiber laser based on a ferroferric-oxide nanoparticles saturable absorber," *Opt. Express* **28**(9), 13177–13186 (2020).
204. S. Y. Set et al., "Laser mode locking using a saturable absorber incorporating carbon nanotubes," *J. Lightwave Technol.* **22**(1), 51–56 (2004).
205. K. Kieu and F. W. Wise, "Soliton thulium-doped fiber laser with carbon nanotube saturable absorber," *IEEE Photonics Technol. Lett.* **21**(3), 128–130 (2009).
206. H. G. Rosa and E. A. T. de Souza, "Pulse generation and propagation in dispersion-managed ultralong erbium-doped fiber lasers mode-locked by carbon nanotubes," *Opt. Lett.* **37**(24), 5211 (2012).
207. Y. Luo et al., "Mode-locked Tm-doped fiber laser based on iron-doped carbon nitride nanosheets," *Laser Phys. Lett.* **14**(11), 110002 (2017).
208. D. Li et al., "Wavelength and pulse duration tunable ultrafast fiber laser mode-locked with carbon nanotubes," *Sci. Rep.* **8**, 2738 (2018).
209. Z. Zhang et al., "Switchable dual-wavelength cylindrical vector beam generation from a passively mode-locked fiber laser based on carbon nanotubes," *IEEE J. Sel. Top. Quantum Electron.* **24**(3), 1100906 (2018).
210. H. Zhang et al., "Large energy soliton erbium-doped fiber laser with a graphene-polymer composite mode locker," *Appl. Phys. Lett.* **95**(14), 141103 (2009).
211. D. Popa et al., "Sub 200 fs pulse generation from a graphene mode-locked fiber laser," *Appl. Phys. Lett.* **97**(20), 203106 (2010).
212. D. Popa et al., "Graphene Q-switched, tunable fiber laser," *Appl. Phys. Lett.* **98**(7), 073106 (2011).
213. H. Mu et al., "Graphene–Bi_2Te_3 heterostructure as saturable absorber for short pulse generation," *ACS Photonics* **2**(7), 832–841 (2015).
214. M. R. Islam et al., "Chronology of Fabry–Perot interferometer fiber-optic sensors and their applications: a review," *Sensors* **14**(4), 7451–7488 (2014).
215. J. Shao et al., "A new hydrogen sensor based on SNS fiber interferometer with Pd/WO_3 coating," *Sensors* **17**(9), 2144 (2017).
216. H. Yan et al., "A fast response hydrogen sensor with Pd metallic grating onto a fiber's end-face," *Opt. Commun.* **359**, 157–161 (2016).
217. C. Yu et al., "Fiber-optic Fabry–Perot hydrogen sensor coated with Pd-Y film," *Photonic Sens.* **5**, 142–145 (2015).
218. Y. Li et al., "Optical cascaded Fabry–Perot interferometer hydrogen sensor based on Vernier effect," *Opt. Commun.* **414**, 166–171 (2018).
219. G. Zhang, M. Yang, and Y. Wang, "Optical fiber-tip Fabry–Perot interferometer for hydrogen sensing," *Opt. Commun.* **329**, 34–37 (2014).
220. S. Tang et al., "Self-compensated microstructure fiber optic sensor to detect high hydrogen concentration," *Opt. Express* **23**(17), 22826–22835 (2015).
221. R. Kitture et al., "Nanocomposite modified optical fiber: a room temperature, selective H_2S gas sensor: studies using ZnO-PMMA," *J. Alloys Compd.* **695**, 2091–2096 (2017).
222. D. Pawar, B. V. B. Rao, and S. N. Kale, "Fe_3O_4-decorated graphene assembled porous carbon nanocomposite for ammonia sensing: study using an optical fiber Fabry–Perot interferometer," *Analyst* **143**(8), 1890–1898 (2018).
223. L. Sansone et al., "Nanochemical fabrication of a graphene oxide-based nanohybrid for label-free optical sensing with fiber optics," *Sens. Actuators B* **202**, 523–526 (2014).
224. M. Debliquy et al., "Optical fibre NO_2 sensor based on lutetium bisphthalocyanine in a mesoporous silica matrix," *Sensors* **18**(3), 740 (2018).
225. M.-J. Yin et al., "Recent development of fiber-optic chemical sensors and biosensors: mechanisms, materials, micro/nano-fabrications and applications," *Coord. Chem. Rev.* **376**, 348–392 (2018).
226. Y.-N. Zhang et al., "Recent advancements in optical fiber hydrogen sensors," *Sens. Actuators B* **244**, 393–416 (2017).

227. D. Pawar, B. V. Bhaskara Rao, and S. N. Kale, "Highly porous graphene coated optical fiber in Fabry-Perot interferometric mode for NH3 gas sensing," in *13th Int. Conf. Fiber Opt. Photon.*, OSA Technical Digest, Tu4A.58 (2016).
228. T. Mak et al., "Optical fiber sensor for the continuous monitoring of hydrogen in oil," *Sens. Actuators B* **190**, 982–989 (2014).
229. A. Aray et al., "Plasmonic fiber optic hydrogen sensor using oxygen defects in nanostructured molybdenum trioxide film," *Opt. Lett.* **44**(19), 4773–4776 (2019).
230. B. Wu et al., "Characteristic study on volatile organic compounds optical fiber sensor with zeolite thin film-coated spherical end," *Opt. Fiber Technol.* **34**, 91–97 (2017).
231. S. Tabassum, R. Kumar, and L. Dong, "Nanopatterned optical fiber tip for guided mode resonance and application to gas sensing," *IEEE Sens. J.* **17**(22), 7262–7272 (2017).
232. J. C. Echeverría, M. Faustini, and J. J. Garrido, "Effects of the porous texture and surface chemistry of silica xerogels on the sensitivity of fiber-optic sensors toward VOCs," *Sens. Actuators B* **222**, 1166–1174 (2016).
233. S. Ruan, H. Ebendorff-Heidepriem, and Y. Ruan, "Optical fibre turn-on sensor for the detection of mercury based on immobilized fluorophore," *Measurement* **121**, 122–126 (2018).
234. X. Zheng et al., "Photochemical modification of an optical fiber tip with a silver nanoparticle film: a SERS chemical sensor," *Langmuir* **24**(8), 4394–4398 (2008).
235. X. Yang et al., "Highly sensitive detection of proteins and bacteria in aqueous solution using surface-enhanced Raman scattering and optical fibers," *Anal. Chem.* **83**(15), 5888–5894 (2011).
236. A. Sanchez-Solis et al., "Print metallic nanoparticles on a fiber probe for 1064-nm surface-enhanced Raman scattering," *Opt. Lett.* **44**(20), 4997–5000 (2019).
237. C. Credi et al., "Fiber-cap biosensors for SERS analysis of liquid samples," *J. Mater. Chem. B* **8**(8), 1629–1639 (2020).
238. J. Zhang et al., "Tapered fiber probe modified by Ag nanoparticles for SERS detection," *Plasmonics* **11**(3), 743–751 (2016).
239. J. Cao, D. Zhao, and Y. Qin, "Novel strategy for fabrication of sensing layer on thiol-functionalized fiber-optic tapers and their application as SERS probes," *Talanta* **194**, 895–902 (2019).
240. J. Shin, B. T. Bosworth, and M. A. Foster, "Single-pixel imaging using compressed sensing and wavelength-dependent scattering," *Opt. Lett.* **41**(5), 886–889 (2016).
241. N. I. Zheludev and Y. S. Kivshar, "From metamaterials to metadevices," *Nat. Mater.* **11**, 917–924 (2012).
242. C. Genet and T. W. Ebbesen, "Light in tiny holes," *Nature* **445**, 39–46 (2007).
243. N. Yu et al., "Light propagation with phase discontinuities: generalized laws of reflection and refraction," *Science* **334**(6054), 333–337 (2011).
244. Z. Zhang et al., "On-fiber plasmonic interferometer for multiparameter sensing," *Opt. Express* **23**(8), 10732–10740 (2015).
245. Y. Liang et al., "A self-assembled plasmonic optical fiber nanoprobe for label-free biosensing," *Sci. Rep.* **9**, 7379 (2019).
246. B. Du et al., "Compact plasmonic fiber tip for sensitive and fast humidity and human breath monitoring," *Opt. Lett.* **45**(4), 985–988 (2020).
247. Y. Wang, F. Liu, and X. Zhang, "Flexible transfer of plasmonic photonic structures onto fiber tips for sensor applications in liquids," *Nanoscale* **10**(34), 16193–16200 (2018).
248. T. Yang et al., "[INVITED] Surface plasmon cavities on optical fiber end-facets for biomolecule and ultrasound detection," *Opt. Laser Technol.* **101**, 468–478 (2018).
249. H. T. Kim and M. Yu, "Lab-on-fiber nanoprobe with dual high-Q Rayleigh anomaly-surface plasmon polariton resonances for multiparameter sensing," *Sci. Rep.* **9**, 1922 (2019).
250. A. Dhawan et al., "FIB fabrication of metallic nanostructures on end-faces of optical fibers for chemical sensing applications," *J. Vac. Sci. Technol. B* **26**(6), 2168–2173 (2008).
251. P. Malara et al., "Resonant enhancement of plasmonic nanostructured fiber optic sensors," *Sens. Actuators B* **273**, 1587–1592 (2018).
252. N. Wang et al., "Nanotrimer enhanced optical fiber tips implemented by electron beam lithography," *Opt. Mater. Express* **8**(8), 2246–2255 (2018).
253. A. Aliberti et al., "Microgel assisted lab-on-fiber optrode," *Sci. Rep.* **7**, 14459 (2017).
254. M. Giaquinto et al., "Optimization strategies for responsivity control of microgel assisted lab-on-fiber optrodes," *Sensors* **18**(4), 1119 (2018).
255. L. Scherino et al., "A time-efficient dip coating technique for the deposition of microgels onto the optical fiber tip," *Fibers* **6**(4), 72 (2018).
256. Y. Zhu, R. A. Dluhy, and Y. Zhao, "Development of silver nanorod array based fiber optic probes for SERS detection," *Sens. Actuators B* **157**(1), 42–50 (2011).
257. M. Consales et al., "Metasurface-enhanced lab-on-fiber biosensors," *Laser Photonics Rev.*, 2000180 (2020).
258. H. E. Arabi et al., "A high throughput supra-wavelength plasmonic bull's eye photon sorter spatially and spectrally multiplexed on silica optical fiber facet," *Opt. Express* **21**(23), 28083–28094 (2013).
259. P. Reader-Harris and A. Di Falco, "Nanoplasmonic filters for hollow core photonic crystal fibers," *ACS Photonics* **1**(10), 985–989 (2014).
260. H. Kim et al., "Metallic Fresnel zone plate implemented on an optical fiber facet for super-variable focusing of light," *Opt. Express* **25**(24), 30290–30303 (2017).
261. H. Kim et al., "Corrugation-assisted metal-coated angled fiber facet for wavelength-dependent off-axis directional beaming," *Opt. Express* **25**(7), 8366–8385 (2017).
262. M. Principe et al., "Evaluation of fiber-optic phase-gradient meta-tips for sensing applications," *Nanomater. Nanotechnol.* **9**, 184798041983272 (2019).
263. J. Yang et al., "Photonic crystal fiber metalens," *Nanophotonics* **8**(3), 443–449 (2019).
264. A. Xomalis et al., "Fibre-optic metadevice for all-optical signal modulation based on coherent absorption," *Nat. Commun.* **9**, 182 (2018).
265. C. Chen et al., "Enhanced optical trapping and arrangement of nano-objects in a plasmonic nanocavity," *Nano Lett.* **12**(1), 125–132 (2012).
266. Y. Pang and R. Gordon, "Optical trapping of 12 nm dielectric spheres using double-nanoholes in a gold film," *Nano Lett.* **11**(9), 3763–3767 (2011).
267. K. Wang et al., "Trapping and rotating nanoparticles using a plasmonic nano-tweezer with an integrated heat sink," *Nat. Commun.* **2**, 469 (2011).
268. A. N. Grigorenko et al., "Nanometric optical tweezers based on nanostructured substrates," *Nat. Photonics* **2**, 365–370 (2008).
269. M. L. Juan et al., "Self-induced back-action optical trapping of dielectric nanoparticles," *Nat. Phys.* **5**, 915–919 (2009).
270. J. M. Ehtaiba and R. Gordon, "Beaming light through a bow-tie nanoaperture at the tip of a single-mode optical fiber," *Opt. Express* **27**(10), 14112–14120 (2019).
271. J. Berthelot et al., "Three-dimensional manipulation with scanning near-field optical nanotweezers," *Nat. Nanotechnol.* **9**, 295–299 (2014).
272. R. M. Gelfand, S. Wheaton, and R. Gordon, "Cleaved fiber optic double nanohole optical tweezers for trapping nanoparticles," *Opt. Lett.* **39**(22), 6415–6417 (2014).
273. A. A. Saleh et al., "Grating-flanked plasmonic coaxial apertures for efficient fiber optical tweezers," *Opt. Express* **24**(18), 20593–20603 (2016).
274. H. Pahlevaninezhad et al., "Nano-optic endoscope for high-resolution optical coherence tomography *in vivo*," *Nat. Photonics* **12**, 540–547 (2018).

275. B.-C. Zheng and F. Xu, "A compact fiber magnetic sensor based on graphene NEMS," in *Asia Commun. Photonics Conf.*, Hong Kong (2015).
276. J. Y. Wu et al., "Broadband MoS_2 field-effect phototransistors: ultrasensitive visible-light photoresponse and negative infrared photoresponse," *Adv. Mater.* **30**(7), 1705880 (2018).
277. W. Choi et al., "High-detectivity multilayer MoS_2 phototransistors with spectral response from ultraviolet to infrared," *Adv. Mater.* **24**(43), 5832–5836 (2012).
278. X. Gan et al., "Chip-integrated ultrafast graphene photodetector with high responsivity," *Nat. Photonics* **7**, 883–887 (2013).
279. F. H. Koppens et al., "Photodetectors based on graphene, other two-dimensional materials and hybrid systems," *Nat. Nanotechnol.* **9**, 780–793 (2014).
280. Q. H. Wang et al., "Electronics and optoelectronics of two-dimensional transition metal dichalcogenides," *Nat. Nanotechnol.* **7**, 699–712 (2012).
281. W. W. Zhao, J. J. Xu, and H. Y. Chen, "Photoelectrochemical DNA biosensors," *Chem. Rev.* **114**(15), 7421–7441 (2014).
282. K. Esquivel et al., "Development of a TiO_2 modified optical fiber electrode and its incorporation into a photoelectrochemical reactor for wastewater treatment," *Water Res.* **43**(14), 3593–3603 (2009).
283. X. T. Zheng et al., "Bifunctional electro-optical nanoprobe to real-time detect local biochemical processes in single cells," *Biosens. Bioelectron.* **26**(11), 4484–4490 (2011).
284. S. Yu et al., "2D materials for optical modulation: challenges and opportunities," *Adv. Mater.* **29**(14), 1606128 (2017).
285. M. Liu et al., "A graphene-based broadband optical modulator," *Nature* **474**, 64–67 (2011).
286. X. Gan et al., "Graphene-assisted all-fiber phase shifter and switching," *Optica* **2**(5), 468–471 (2015).
287. J.-H. Chen et al., "An all-optical modulator based on a stereo graphene–microfiber structure," *Light Sci. Appl.* **4**, e360 (2015).
288. I. V. Fedotov et al., "Fiber-optic magnetic-field imaging," *Opt. Lett.* **39**(24), 6954–6957 (2014).
289. I. V. Fedotov et al., "High-resolution magnetic field imaging with a nitrogen-vacancy diamond sensor integrated with a photonic-crystal fiber," *Opt. Lett.* **41**(3), 472–475 (2016).
290. S. M. Blakley et al., "Room-temperature magnetic gradiometry with fiber-coupled nitrogen-vacancy centers in diamond," *Opt. Lett.* **40**(16), 3727–3730 (2015).
291. I. V. Fedotov et al., "Electron spin manipulation and readout through an optical fiber," *Sci. Rep.* **4**, 5362 (2014).

Yifeng Xiong is a PhD candidate of the College of Engineering and Applied Sciences at Nanjing University, under the supervisor of professor Fei Xu. He received his BEng degree in materials physics from Nanjing University. His current research focuses on integrated optical fiber devices.

Fei Xu is a professor at the College of Engineering and Applied Sciences, Nanjing University, Nanjing, China. He received his PhD from Optoelectronics Research Center, University of Southampton, UK, in 2008. His research interests include fiber optics.